



Aalborg Universitet

AALBORG UNIVERSITY
DENMARK

Multichannel electrotactile stimulation to restore full-state sensory feedback in myoelectric hand prostheses

Garenfeld, Martin Alexander

DOI (link to publication from Publisher):
[10.54337/aau561809161](https://doi.org/10.54337/aau561809161)

Publication date:
2023

Document Version
Publisher's PDF, also known as Version of record

[Link to publication from Aalborg University](#)

Citation for published version (APA):
Garenfeld, M. A. (2023). *Multichannel electrotactile stimulation to restore full-state sensory feedback in myoelectric hand prostheses*. Aalborg Universitetsforlag. <https://doi.org/10.54337/aau561809161>

General rights

Copyright and moral rights for the publications made accessible in the public portal are retained by the authors and/or other copyright owners and it is a condition of accessing publications that users recognise and abide by the legal requirements associated with these rights.

- Users may download and print one copy of any publication from the public portal for the purpose of private study or research.
- You may not further distribute the material or use it for any profit-making activity or commercial gain
- You may freely distribute the URL identifying the publication in the public portal -

Take down policy

If you believe that this document breaches copyright please contact us at vbn@aub.aau.dk providing details, and we will remove access to the work immediately and investigate your claim.

**MULTICHANNEL ELECTROTACTILE
STIMULATION TO RESTORE FULL-STATE
SENSORY FEEDBACK IN MYO-ELECTRIC
HAND PROSTHESES**

**BY
MARTIN ALEXANDER GARENFELD**

DISSERTATION SUBMITTED 2023



AALBORG UNIVERSITY
DENMARK

MULTICHANNEL ELECTROTACTILE STIMULATION TO RESTORE FULL- STATE SENSORY FEEDBACK IN MYO- ELECTRIC HAND PROSTHESES

by

Martin Alexander Garenfeld



AALBORG UNIVERSITY
DENMARK

Dissertation submitted June 2023

Dissertation submitted: June 2023

PhD supervisor: Prof. Strahinja Dosen,
Aalborg University

Assistant PhD supervisor: Associate Prof. Jakob Lund Dideriksen,
Aalborg University

PhD committee: Associate Professor Anderson
de Souza Castelo Oliveira (chair)
Aalborg University, Denmark

Professor Stanisa Raspopovic
ETH Zürich, Switzerland

Professor Christian Cipriani
Sant'Anna School of Advanced Skills - Pisa, Italy

PhD Series: Faculty of Medicine, Aalborg University

Department: Department of Health Science and Technology

ISSN (online): 2246-1302
ISBN (online): 978-87-7573-681-2

Published by:
Aalborg University Press
Kroghstræde 3
DK – 9220 Aalborg Ø
Phone: +45 99407140
aauf@forlag.aau.dk
forlag.aau.dk

© Copyright: Martin Alexander Garenfeld

Printed in Denmark by Stibo Complete, 2023



CV

Martin received his undergraduate and master's degree in biomedical engineering from Aalborg University in 2017 and 2019, respectively. Following graduation, Martin continued the academic path at Aalborg University and has since July 2019 been a PhD student in the Neurorehabilitation Systems research group at the Department of Health Science and Technology supervised by Professor Strahinja Dosen and co-supervised by Associate Professor Jakob Lund Dideriksen. The PhD project focused on the intuitive communication of somatosensory information of multifunctional myoelectric hand prostheses. Parallel to the PhD project, Martin has been involved in additional activities of contributing to the EU-funded projects TACTILITY and SIXTH SENSE, submitting and publishing studies outside the PhD project, reviewing manuscripts, acting as a panelist and presenter at webinars and workshops and participating in teaching activities including semester coordination, guest lecturing and co-examining at project exams.

PREFACE

This thesis disseminates the entire work produced during the PhD project of Martin Alexander Garenfeld in the research group of Neurorehabilitation Systems at the Department of Health Science, Aalborg University in the period from year 2019 to 2023. The work is published in established peer-reviewed scientific journals:

- [1] M. A. Garenfeld, C. K. Mortensen, M. Strbac, J. L. Dideriksen, and S. Dosen, “Amplitude versus spatially modulated electrotactile feedback for myoelectric control of two degrees of freedom,” *J. Neural Eng.*, vol. 17, no. 4, pp. 1–15, 2020.
- [2] M. A. Garenfeld et al., “A compact system for simultaneous stimulation and recording for closed-loop myoelectric control,” *J. Neuroeng. Rehabil.*, vol. 18, no. 1, pp. 1–17, 2021.
- [3] M. A. Garenfeld, M. Strbac, N. Jorgovanovic, J. L. Dideriksen, and S. Dosen, “Closed-Loop Control of a Multifunctional Myoelectric Prosthesis With Full-State Anatomically Congruent Electrotactile Feedback,” *IEEE Trans. Neural Syst. Rehabil. Eng.*, vol. 31, pp. 2090–2100, 2023.

The thesis content is structured into six chapters. Chapter 1 outlines the current technology for upper limb prosthesis users and discusses the role of sensory feedback in estimating motor control actions. An overview of the current literature regarding closed-loop sensorimotor control of myoelectric prostheses is provided and analyzed to conceptualize the aim of the project and define the research questions to address. Chapter 2 describes the equipment used in the project, and Chapter 3 explains the methods applied to implement pattern-recognition based control of myoelectric prostheses as well as challenges and implementation decisions that were considered. Chapter 4 explains the novel electrotactile feedback encodings to communicate the state of the prosthesis. Chapter 5 describes how the performance of the myoelectrical control was evaluated and Chapter 6 describes the experimental protocols and reports and discusses the outcome of the three studies comprising the project. Chapter 7 synthesizes the work by answering the posed research questions to form conclusions and provide a perspective on future challenges.

ENGLISH SUMMARY

A transradial amputation is a dramatic event that causes a substantial loss of motor and sensory functions. The state-of-the-art myoelectrically controlled prostheses can be used to restore the lost motor function. However, despite the technological developments in mechatronics, many prosthesis users still abandon their devices due to several factors, from ergonomics and difficulties in control to the lack of somatosensory feedback from the prosthesis. The feedback can be restored using mechanical or electrical stimulation, but most of the studies in the literature focus on simple prosthetic devices with a single function (open/close). However, modern prostheses are advanced robotic systems that encompass multiple degrees of freedom, and therefore, several feedback variables need to be simultaneously communicated back to the user to effectively close the loop and convey the full state of the system. Electrotactile stimulation using surface electrodes is a non-invasive feedback strategy that can integrate many stimulation channels into a compact system. The aim of the present thesis was therefore to investigate how this approach can be used to convey multivariable feedback that is clear to perceive and easy to interpret.

To this aim, the present PhD project investigated different feedback encoding schemes to represent the states of a multifunctional prosthesis and validated the feasibility of simultaneous electrotactile stimulation and myoelectric recording for stable closed-loop myoelectric control. The first study demonstrated that both spatially and intensity modulated feedback configurations intuitively conveyed discrete information regarding hand aperture and wrist rotation of a virtual myoelectric prosthesis controlled using myoelectric signals from the contra-lateral forearm to avoid interference. When placing stimulation and recording electrodes on the same arm, however, the stimulation pulses contaminate the recorded electromyography which disturbs the prosthetic control. Therefore, in the second study, a compact system for simultaneous recording and stimulation with integrated artefact blanking mechanism was presented and the closed-loop control of a virtual prosthesis was further evaluated with the stimulation and recording electrodes placed ipsilaterally. The same setup was used in the last study to communicate the full state of a physical prosthesis (aperture, rotation, and grasp force) during functional prosthesis use. A novel mapping was proposed that generated tactile sensations which were anatomically congruent to prosthesis motions. The results from a functional task indicated that the novel feedback improved prosthesis control performance compared to the condition in which electrotactile stimulation was deactivated.

In summary, the main contributions of the present thesis are the technical development of compact solutions for closed-loop prosthesis control, design of effective encoding schemes for multivariable feedback, and the assessment of human perception and benefits of such feedback. These are important steps towards clinical applications of modern prostheses enhanced with sensory feedback.

DANSK RESUME

En transradial amputation er en traumatisk hændelse, der medfører betydeligt tab af motorisk og sensorisk funktionalitet. De nyeste myoelektrisk styrede proteser udgør teknologier som kan være med til at erstatte den mistede motoriske funktion. Til trods for den store teknologiske udvikling af protesens mekatroniske komponenter vælger mange brugere myoelektriske proteser fra, af årsager som brugsbekvemmelighed, besvær med styringen og manglende somatosensorisk feedback. Selve feedbacken kan blive genskabt for eksempel ved at stimulere mekanisk eller med en svag strøm på huden. De fleste studier har fokuseret på proteser med en simpel bevægelighed af en enkelt frihedsgrad (åben og lukke funktion), men moderne proteser har en bevægelighed der udgør flere frihedsgrader, hvilket kræver at adskillige feedbackvariabler samtidigt skal kommunikeres for at den sensoriske funktionalitet imødekommer den motoriske. Elektrotaktile stimulation er en lovende, ikke-invasiv feedback teknik der kan indbefatte mange stimuleringskanaler i et kompakt system, men kan dog medføre problemer med styringen af den myoelektriske protese grundet elektrisk interferens. Formålet med dette PhD projekt var derfor at undersøge, hvordan elektrotaktile feedback kan bruges til at kommunikere flere feedbackvariabler samtidigt, på en måde, der er let at opfatte og let kan fortolkes til brugbar information.

Forskellige feedback konfigurationer blev udviklet til at beskrive protesens multifunktionelle tilstande, og det blev valideret, hvordan elektrotaktile stimulation kan anvendes sammen med myoelektriske signal til stabil styring af protesen. Det første studie viste at både spatiel og intensitetsmodulerede feedback konfigurationer let forståeligt kan kommunikere diskret information vedrørende en virtuel myoelektrisk proteses håndåbning og håndledsrotation når stimuleringen leveres på modsatte underarm for at undgå interferens. Den andet studie validerede brugen af et kompakt system, der kan muliggøre simultan myoelektrisk signal optagelse og elektrotaktile stimulation på samme underarm og samtidig understøtte stabil styring af en virtuel protese. I det tredje og sidste studie blev det samme system brugt til at kommunikere den fulde funktionalitet af en rigtig fysisk multifunktionel protese (håndåbning, håndledsrotation og grebsstyrke) gennem en funktionel test. En original feedback konfiguration blev udviklet, hvor den elektrotaktile stimulation bevægede sig synkroniseret med protesens bevægelser. Resultaterne indikerede, at informationerne indeholdt i den originale elektrotaktile feedback forbedrede forsøgspersonernes styring af protesen sammenlignet med at styre protesen på konventionel vis (ingen elektrotaktile feedback).

Som opsummering var hovedbidragene i dette PhD projekt validering af et kompakt system til understøttelse af simultan brug af elektrotaktile stimulation og stabil myoelektrisk protesestyring, udvikling af brugbare konfigurationer kommunikation af multivariabel feedback og evalueringen af brugerens opfattelse og anvendelighed af feedbacken. Dette er et vigtigt skridt hen mod klinisk anvendelse af multifunktionelle moderne proteser understøttet med sensorisk feedback.

ACKNOWLEDGEMENTS

My mother is a lady of many fitting phrasings and pronouns. Throughout my academic endeavors the saying “for at virke lært, skal man gøre det lette svært” has occasionally been uttered. A non-rhyming, dissonant English translation sounds: “to seem knowledgeable, the easy must be made difficult”. While most likely just being a mocking remark on my ability to explain what my research is about, the saying itself can also be interpreted as a critique of the “intellectual field” only nitpicking insignificant details without adding proper value. Admittedly, the feeling of irrelevance has also crossed my mind now and then when reflecting on the work I have been conducting for my PhD; that the world would have been more or less unchanged without the presence of my findings. Rewinding the downward spiral of these rather unconstructive thoughts, I came to the realization that they were a product of setting too high expectations for the impact of my work. While about four years is a long time, it is a short duration to produce groundbreaking scientifically validated results in biomedical engineering, especially when you are quite alone in conducting most elements of the research: conceptualizing, interfacing hardware, implementing software, pilot testing, iterating, collecting data, analyzing data, documenting, reflecting, justifying. And exactly this attention to detail and investigation of aspects blind to the untrained eye are what knit together the robustness and beauty of science. “Mange bække små, gør en stor å”: “Many small streams form a great river”. So, I do feel content with the grand effort of the PhD project despite not having moved any mountains, but maybe some gravel somewhere. And I do feel grateful on a personal level for the opportunity of experiencing the PhD and all the invaluable insights it has brought.

With that said, as this section is actually dedicated to acknowledgements and not relentless self-centered ramble, I will first mention my supervisor Strahinja, who made this PhD experience possible. I highly appreciate your engagement in ensuring that everything functions in every aspect of the process. I think it is rare to have a senior supervisor who will actually sit with you in the lab and troubleshoot on code-level. But mostly thank you for being such an empathetic and easy-going person with a great sense of humor. Also, thank you to Jakob, my co-supervisor, who has actually been a part of my academic endeavors since the beginning of the Bachelor. You have been a splendid team of supervisors.

A huge thanks goes to all the other people at the University for great scientific sparring, lunch talks and social activities. I admit having neglected the latter part following the Covid lockdown and especially after becoming a father which required a restructuring of priorities. A special thanks to Mauri, Marco, and Luis for always being ready to talk bullshit and for your relatable personas. Also, thanks to Mads and Bas for some great first two years in- and outside UniFitness.

I dedicate my work to the dearest love of my life and main source of inspiration, my muse, Hulda. Clichély put, I would not have been able to finish the work without you. You have helped me soothe away all frustrations and truthfully expanded my knowledge more than the PhD studies have during this period of time. And I endlessly thank you for bringing our perfect son, Isak, into the world. I could not be happier than I am knowing I have the two of you by my side. I love you both to the moon and back. Lastly, all the thanks go to my parents for your unconditional support and loyalty. I cannot emphasize how grateful I am for everything you have done for me. This is just as much your achievement as it is mine.

TABLE OF CONTENTS

Chapter 1. Introduction	13
1.1. Implications of hand amputation.....	13
1.2. Prosthesis solutions.....	13
1.2.1. Passive prostheses.....	13
1.2.2. Body-powered prostheses.....	15
1.2.3. Electrically powered prostheses.....	15
1.3. Somatosensory feedback restoration.....	16
1.3.1. Somatotopical feedback.....	17
1.3.2. Modality-matched feedback.....	18
1.4. Substitution feedback.....	18
1.4.1. Vibrotactile stimulation.....	18
1.4.2. Electrotactile stimulation.....	19
1.4.3. Electrical artefact suppression.....	21
1.4.4. Communication of multiple feedback variables.....	22
1.5. Aim of the project.....	24
1.5.1. Research questions.....	25
Chapter 2. Equipment	27
2.1. Myo armband.....	27
2.2. MaxSens device.....	27
2.2.1. EMG recording.....	27
2.2.2. Electrotactile stimulation.....	29
2.2.3. Stimulation artefact blanking.....	29
2.3. Michelangelo Hand.....	31
Chapter 3. Myoelectric prosthetic control	33
3.1. Myoelectric control using pattern recognition.....	33
3.2. Recording equipment.....	34
3.3. Data segmentation.....	35
3.4. Signal processing.....	35
3.5. Feature extraction.....	38

3.6. Training data acquisition.....	38
3.7. Pattern recognition and proportional control.....	39
Chapter 4. Electrotactile stimulation to communicate somatosensory feedback	41
4.1. Stimulation intensity calibration	41
4.2. Spatial versus amplitude modulation	42
4.3. Mixed encoding.....	44
4.4. COMMUNICATING full state of prosthesis.....	45
Chapter 5. Tasks for evaluation of myoelectric control performance	47
5.1. Online prosthetic control and mapping	47
5.2. Training understanding of feedback.....	48
5.3. Virtual target reaching task	50
5.4. Multifunctional prosthesis task	51
5.5. Statistical analysis	51
Chapter 6. Main results	53
6.1. Two-DoF position information can be provided effectively through either spatial or amplitude modulated electrotactile feedback	53
6.2. Firmware blanking of stimulation artefacts facilitates stable closed-loop myoelectric control when placing electrodes ipsilaterally	57
6.3. Provision of supplementary feedback during myoelectric control improves position estimation of a multifunctional prosthesis.....	59
Chapter 7. Conclusions	62
7.1. Future challenges	64
Chapter 8. Literature list	67

CHAPTER 1. INTRODUCTION

1.1. IMPLICATIONS OF HAND AMPUTATION

The human hands are highly dexterous manipulation tools driven by anatomical features (multiple joints and muscles) that allow effortless control of numerous degrees of freedom (DoFs), 21 and 3 in the fingers and wrist, respectively. The physiological properties of the forearm and hands allow the hands to move dexterously and perform a wide range of movements, from delicate and precise to powerful. The precise motion is largely shaped by rich sensory information detected by receptors and analyzed by the brain to form a closed-loop motor response [4]–[8] (see flow of motor and sensory signals on left side of *Fig. 1a*). While auditory and especially visual feedback play important roles in determining movements, somatosensory feedback is required for optimal sensorimotor control [9]. The insight into human anatomy demonstrates the importance of somatosensory information for motor execution as sensory axons in all nerves innervating the arm and hand outweigh the motor axons by at least 1:9 [10]. The available tactile and proprioceptive information are simultaneously evaluated to perform the best possible motor action given the intention and situation [4]. This sophisticated interaction between somatosensory input and motor output makes the hands an essential tool in almost all activities of daily life and social interactions and facilitates higher level of independence [11], [12].

A loss of the hand is therefore a debilitating event that can affect occupational status [11], self-image and create a sense of feeling different [12] negatively impacting life satisfaction [11]. An estimated 57.7 million people globally are living with traumatic limb amputation [13] with 1:4-5 occurring in upper limb and 70 % of those below the elbow (trans-radial and further distally) [14], [15]. As an effort to minimize negative psychological and physiological impact, the trans-radial amputee can wear a prosthesis – a replacement of the loss limb. A wide range of prosthesis solutions can be provided with varying levels of functionality.

1.2. PROSTHESIS SOLUTIONS

Prosthetic devices for trans-radial amputees can be divided into three main classes: passive, body-powered, and myoelectric.

1.2.1. PASSIVE PROSTHESES

A passive prosthesis consists of a naturally looking replicate of the missing hand or an assistive tool [16]. While the former option mainly serves to restore appearance, a passive hand created with a flexible design can also grasp objects below a certain weight by pushing the object with the prosthesis against an opposing force, e.g., intact

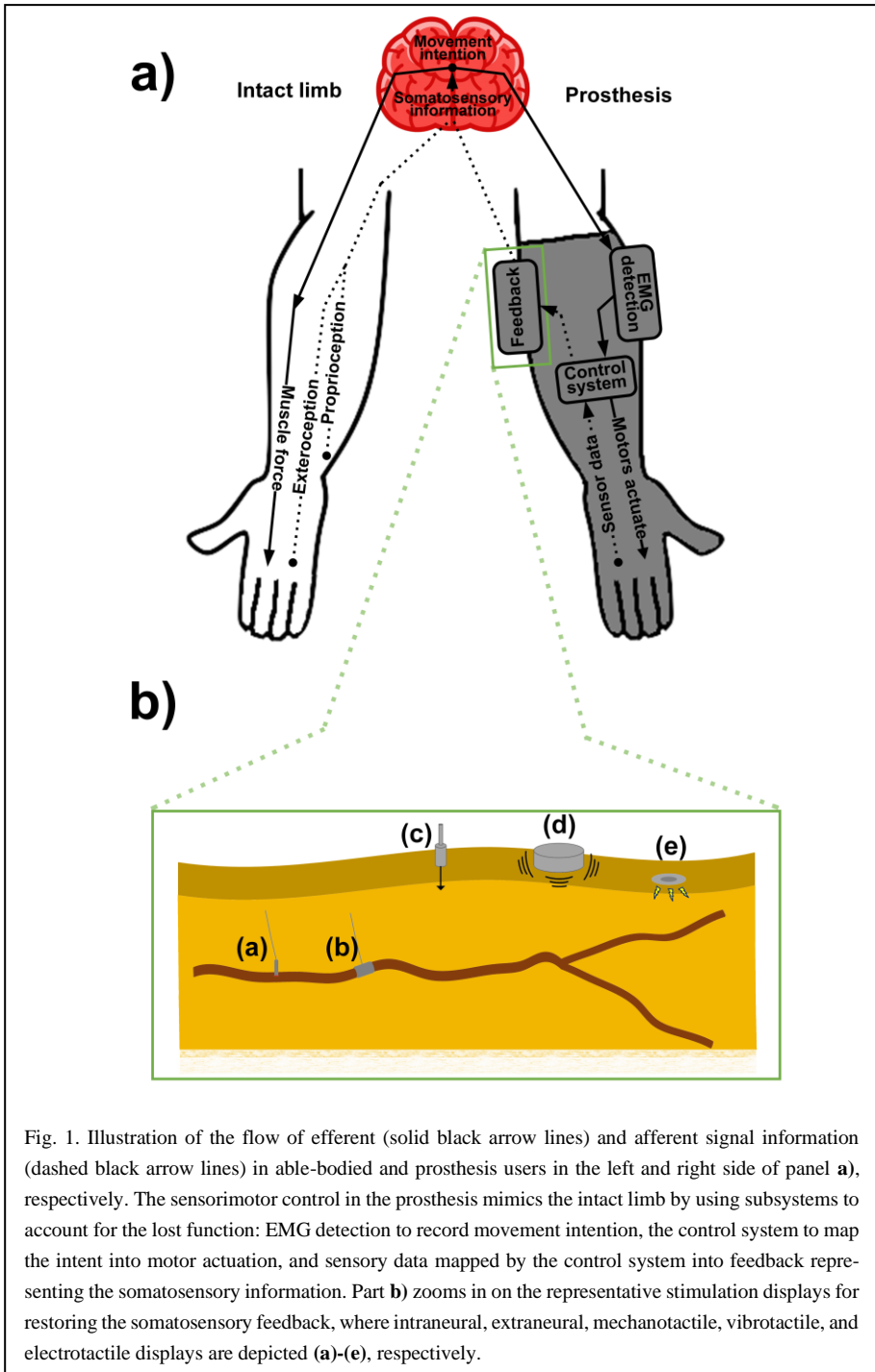


Fig. 1. Illustration of the flow of efferent (solid black arrow lines) and afferent signal information (dashed black arrow lines) in able-bodied and prosthesis users in the left and right side of panel a), respectively. The sensorimotor control in the prosthesis mimics the intact limb by using subsystems to account for the lost function: EMG detection to record movement intention, the control system to map the intent into motor actuation, and sensory data mapped by the control system into feedback representing the somatosensory information. Part b) zooms in on the representative stimulation displays for restoring the somatosensory feedback, where intraneural, extraneural, mechanotactile, vibrotactile, and electrotactile displays are depicted (a)-(e), respectively.

hand or surrounding environment [17]. When performing specific activities, assistive tools can be attached to the residual limb to support the use of cooking aids and utensils, sporting equipment, musical instruments etc. [18], [19]. However, assistive tools are a less common prosthesis choice as the adjustable passive hand offers a similar functionality for most daily life activities, while retaining a natural appearance [16].

1.2.2. BODY-POWERED PROSTHESES

A body-powered prosthesis has less emphasis on appearance but provides the user with an active end-actuator, or gripper, driven by a cable connected to the contralateral shoulder [20]. This system provides a single DoF as pulling the cable closes and opens the gripper. In addition, a direct connection between the shoulder and the gripper provides the user with proportional tactile feedback regarding the grasping force (so called, extended physiological proprioception) [21]. The control of the cable-driven prosthesis is precise, but the system can be more unpleasant to utilize over longer periods of time as more gross limb movements are needed and constant muscle tension must be applied to maintain grasping force [22].

1.2.3. ELECTRICALLY POWERED PROSTHESES

Electrically powered prostheses employ an outside power source to generate energy to move the end-effector. Most electrical prostheses are controlled intuitively via surface electromyographic (EMG) signals produced by the user. The EMG signal is a superposition of motor unit action potentials propagating along the muscle fibers [23]. EMG is generated in response to the subject's intention to perform a movement and therefore provides means for intuitive control (e.g., the subject thinks about hand opening and the prosthesis opens). The prosthesis control is most commonly proportional and velocity-based, meaning that the velocity of prosthesis movement and the force generated after contact are proportional to the EMG signal amplitude, and the position (force) is maintained during rest [24]. Thus, the user is relieved from the need to sustain the muscle contraction when the desired prosthesis position/force is reached, contrary to the control of the body-powered prosthesis. With the recent advances in mechatronics, some commercially available prostheses allow movement across multiple DoFs approximating the dexterity of the biological hand [25]. However, most often simple switch-based myoelectric control is applied in these advanced devices. EMG signals are recorded from agonist-antagonist muscles (e.g., flexor-extensor) on the residual forearm, and then one muscle regulates one direction of the active prosthesis joint and vice versa for the other. A switch signal is produced to change the active DoF, e.g., co-contraction of the two muscles groups. The muscle activation is therefore not necessarily mapped to the equivalent prosthesis joint movement, and it can be more cumbersome to navigate between multiple DoFs [26]. Pattern recognition control translates instead the muscle contraction pattern into the matching prosthesis movement [27]. EMG signals are recorded from multiple sites around the residual limb, and the pattern recognition system then evaluates the signal information

to identify the user's intended gestures. The user can then more intuitively shift between DoFs. Most commonly, pattern recognition systems utilize classification to facilitate sequential control of a single DoF at a time and is applied in a few commercially available products [28], [29]. Simultaneous control of multiple DoFs similar to natural movement of the biological hand can be realized by using regression models [30], [31]. Despite the increased naturalness and utility of combining movement of several DoFs [32], [33], simultaneous control is still confined to research.

Despite the wide variety of prosthetic solutions, as many as 20-50 % upper-limb amputees still choose to abandon the provided prosthesis with frequent reasons being uncomfortable fit and poor functionality [34]–[36]. Especially some unilateral amputees prefer to predominantly use their sound side to perform daily life activities instead of wearing prostheses [37]–[39]. They find that activities of daily life can be completed efficiently with substitutive use of the sound limb and other body parts (chin, mouth, lower limb) [40]. However, compensatory behavior can lead to the risk of overuse and injury of the intact limb and other sound body parts, which could be avoided by using a prosthesis to relieve the excessive one-sided load [41], [42]. Body-powered and myoelectric devices best supply the needed functionality, and they are also the favored prosthesis choice amongst users [36], [43].

Disregarding current practical obstacles (mounting time, calibration time, maintenance, battery-life, external load), pattern recognition-based myoelectrically controlled prostheses have the potential of restoring the lost functional dexterity most naturally (high cosmeses [43], [44], multi-DoF motion, and intuitive control interface [45]). Therefore, pattern recognition prosthetic control was applied in the present PhD project.

1.3. SOMATOSENSORY FEEDBACK RESTORATION

Somatosensory feedback consists of abundant sensory information comprising touch (roughness, hardness, moistness, slipperiness) [46], temperature, nociception (pain), itching, tickling, pressure, and proprioception (joint angles, limb position). While body-powered prostheses provide moderate proportional force feedback, myoelectric prosthesis users only receive unintentional sounds and mechanical vibration from actuation motors [47]. This incidental feedback provides indirect information about e.g., prosthesis velocity, DoF-switch, and even grasping force and this has shown to be useful for prosthesis control [48]. Other available sources (intrinsic feedback) to estimate the state of the prosthesis are e.g., the contraction intensity and duration, joint torque and skin friction. However, without informative somatosensory feedback, the amputee still needs to rely more heavily on visual feedback to estimate movements [49], [50]. While studies have shown improved performance using supplementary feedback describing information somewhat available through vision, e.g., grasp force [51], [52], other approaches improved performance by conveying information that

was not directly assessable through visual feedback, e.g., discrete events (object contact and release) [53], [54], EMG amplitude (muscle contraction) [55], pattern classification error [56]. When the incidental feedback was eliminated by controlling a virtual prosthesis (digital representation of a prosthesis), further studies have shown an improvement in task performance with added supplementary feedback while receiving visual cues [57]–[59]. Vision is a rich source of information during sensorimotor control [4] but can be occluded in various daily life activities, e.g., grasping a glass in a cupboard. In such cases, supplementary somatosensory feedback can contribute even more substantially to improving control performance [60]–[63].

Specifically, myoelectric prosthesis users have expressed main interest in receiving the feedback variables describing the prosthesis' state: grasp force and prosthesis position (hand aperture and wrist rotation) [64], [65]. **However, for the supplementary feedback to be useful for the prosthesis user, it must be clear to the user and more informative than the incidental and intrinsic feedback sources already available [4], [66], [67]. Comparing the myoelectric control performance when receiving only on the incidental feedback versus adding supplementary feedback regarding the prosthesis' state is rarely addressed in the literature.** In order for an accurate representation of the prosthesis' state to be communicated to the user, prosthesis sensor data needs to be mapped into stimulation profiles and provided to the user [5], see right side of *Fig. 1a*. The provision of somatosensory feedback to close the loop in prosthetic control can be achieved using various stimulation strategies that can be divided into three main categories: somatotopical, modality-matched, and substitution feedback.

1.3.1. SOMATOTOPICAL FEEDBACK

The feedback can be somatotopical, when it is perceived as originating from the phantom limb, which supposedly requires less cognitive processing to interpret [7]. One approach is to outline the amputee's phantom limb map. Specifically, amputees have skin sites on their residual limb referred to as phantom digits that when stimulated activate areas in the brain the evoke sensations corresponding to the missing fingers [68]. However, this method entails time-demanding calibration to identify the specific skin sites that create this phantom limb map. Another approach to evoke somatotopical sensations by superficial stimulation is to activate large peripheral nerves by placing electrodes on the skin above the nerves [69]–[71]. More commonly, direct stimulation of peripheral nerves [72]–[74] or somatosensory cortex [75], [76] are implemented either by penetrating the nerves (intraneural) or by placing the electrodes around the nerves (extraneural) using e.g., cuff electrodes, see *Fig. 1b(a)* and *(b)* for visual illustration. While these invasive approaches show to restore robust bidirectional communication between prosthesis and user [6], they require surgical intervention and this always entails potential risks. This is a main obstacle amongst prosthesis users to utilize such feedback methods [77], [78].

1.3.2. MODALITY-MATCHED FEEDBACK

Modality-matched feedback represents a sensation that is perceived as identical to that provided by the feedback variable (e.g., force conveyed as force applied to the residual limb). Direct peripheral nerve stimulation can theoretically incite all somatosensory sensations somatotopically as the action potentials created by the stimulation travel to the brain for interpretation, same as physiological electrical signals transmitted through afferent nerves [6], [22]. However, the stimulation technology and knowledge about biological processes of translating stimulation into sensation is yet too limited to produce genuine sensations that feel natural. Pressure detected by the sensor in the prosthetic hand can be accurately represented by applying force to the skin of the residual limb (mechanotactile stimulation) using a pushing mechanism [51], see *Fig. 1b(c)*, air-mediated pressure in silicone pads [79] or a pressure cuff [80]. Proprioceptive information regarding hand opening can be represented through skin-stretch [81]. In such cases, the sensation modality is matched but the location is mismatched. While requiring less cognitive processing to interpret compared to other stimulation displays [5]–[7], mechanotactile systems are still overly bulky, power-consuming, and noisy.

1.4. SUBSTITUTION FEEDBACK

One of the major challenges in designing a closed-loop prosthesis solution that also provides the user with adequate somatosensory information, is to fit all hardware components (e.g., EMG electrodes, stimulation display, sensor units, prosthesis actuation motors, batteries, microcontrollers) in a single unit (prosthesis and socket) while remaining light, enabling long duration per charge, and being comfortable to wear [5]. Modality-matched feedback technologies are difficult to provide in a compact solution and they can drain batteries quickly. Alternatively, sensory substitution systems can be used, where the missing sensory input is substituted by translating it into another sense (e.g., touch to audio [82], [83]) or modality (e.g., touch to vibration). The latter approach includes technologies such as electroactive polymers, piezoelectric actuators, and ultra-sound, [84], [85] and more commonly vibro- and electrotactile stimulation [86]. Especially the two latter displays meet the criteria of low power consumption and compactness for easy integration in the prosthesis socket.

1.4.1. VIBROTACTILE STIMULATION

Vibrotactile stimulation is produced by superficially placed vibration motors that activate mechanoreceptors in the skin [86], see *Fig. 1b(d)* for visual representation. The stimulation can be modulated in amplitude and frequency (sinusoidal wave) that affect the intensity and quality of sensation, respectively. Even though only two physical parameters can be modulated, several perceived sensations can be created from modulating a single parameter [87]. For instance, at least three distinct sensations can be perceived by modulating frequency (static pressure, flutter, and smooth vibration), but these sensations can also be identified when the stimulation signal contains multiple

frequencies [88]. Thus, three perceived sensations can be generated by modulating a single physical parameter. The stimulation can be additionally modulated temporally and spatially to shape the feedback. Temporal modulation of the stimulation duration (on/off) can be applied to create temporal patterns or rhythms [89], [90]. Multiple factors can also be combined in a single stimulation display (an array or matrix), which allows spatial modulation (changing location of stimulation by activating different motors) [91]–[93], but also generation of tactile spatial patterns through simultaneous activation of several motors [89], [94]. Hence, vibrotactile stimulation can exploit multiple stimulation modulations to communicate the prosthesis’ state and more sophisticated somatosensory information.

These strategies have been used to convey different feedback variables to the user of a prosthesis. For instance, stimulation amplitude was modulated to convey discrete information about hand aperture [60], [61], [95], prosthesis velocity [96], grasp force [97] and this approach was also combined with spatial coding to implement grasp force feedback [52], [98]. Spatial modulation was used to represent levels of hand aperture [99], [100], grasp force [101]–[104], EMG amplitude (muscle contraction intensity) [101]–[103] and it was combined with temporal modulation for communicating contact and DoF-switch [52]. Temporal modulation alone was used to communicate grasp force [99], [105] and discrete events (contact/release) [54], [66].

Vibrotactile feedback has been already introduced in a few commercial prostheses [106]–[108] but using only a single factor conveying a single feedback variable. However, vibrotactile technology poses several disadvantages. The stimulation amplitude and frequency cannot be modulated entirely independently as the two parameters are coupled mechanically (i.e., by a resonance effect) [109]. Also, each factor contains a motor and this limits the miniaturization of the technology and the practical integration of multiple factors inside the prosthesis socket for spatial modulation [52], [98]–[104].

1.4.2. ELECTROTACTILE STIMULATION

Electrotactile stimulation delivers low-amplitude current from an electrode placed on the skin surface to directly activate afferent nerves that are associated with mechanoreceptors [110], see *Fig. 1b(e)* for visual representation. Most commonly, sensation is designed to be produced below what is referred to as the active pad(s) while the reference pad ideally does not produce sensation but is required to close the electrical circuit. This is achieved by making the reference pads larger, thereby decreasing the current density to minimize the activation of the skin afferents [110], [111]. The sensation of electrotactile stimulation has been subjectively described as “a tingle, itch, vibration, buzz, touch, pressure pinch and sharp and burning pain, depending on the stimulation voltage, current, and waveform, and the electrode size, material, contact force, skin location, thickness, and hydration”, quoted from [86]. To reduce the risk

of pain or unpleasant sensations, simple precautions can easily be taken: deliver biphasic pulses to avoid skin-reddening [110], cleanse and moisturize the skin to lower and even out skin impedance (current flows through areas of low resistance), ensure a close and stable skin-electrode contact (electrode peeling off decreases contact size and increase current density), and carefully calibrate the stimulation intensity before use (avoid recruitment of nociceptors and ensure homogenous intensity across all electrode pads) [86], [110], [112], [113]. Thus, reasons for the more frequency use of vibrotactile is likely due to fast calibration of sensation intensity, the familiarity of sensing mechanical vibration, and low risk of recruiting nociceptors (painful sensations) [114]. However, as the vibrotactors contain mechanical moving parts opposed to electrotactile stimulation, vibrotactile stimulation also responds slower, produce incidental noise, and consume more power.

The electrotactile stimulation can be modulated similarly as vibrotactile stimulation: intensity (amplitude or pulse width modulation), frequency, temporal modulation, and location of stimulation. Contrary to vibration interfaces, multiple frequencies cannot be combined into a complex periodic signal, but the effect can be somewhat reproduced by using simultaneous modulation of frequency and temporal length [115]. Opposed to vibrotactile stimulation, the intensity and frequency are decoupled and can be independently modulated. When using an electrode with multiple active pads (stimulation channels), the frequency, however, is a common parameter. The electrode can be easily fabricated, and stimulation pads can be customized into any shape, size and spatial arrangement [116]. The active pads can therefore be densely packed, where density is only limited by the two-point discrimination (8.93 mm for the forearm) [117], [118]. The independently adjustable physical parameters (intensity and frequency) and compactly distributed stimulation pads facilitate a stimulation display with higher bandwidth for information transfer compared to vibrotactile stimulation. Furthermore, a slim electrode, miniature stimulation device [116], low power-consumption, and no noise from mechanical moving parts make an electrotactile system suitable for placing inside the socket, thereby enabling a practical and wearable closed-loop prosthetic system. Therefore, electrotactile stimulation was selected in the present PhD project as a technology of choice to communicate somatosensory feedback for closed-loop myoelectric control.

Electrotactile feedback has been used before to represent feedback variables from a prosthesis. Spatial modulation was employed to communicate grasping force [67], [119], hand aperture, and wrist rotation [116], and this approach was also mixed with frequency modulation to convey grasp force [55], [67], [120] and EMG amplitude [55]. Modulating amplitude [100] and pulse width [57], as well as frequency and temporal modulation was used to transmit grasp force and wrist flexion/extension, respectively [116]. As also indicated by the literature overview for vibrotactile stimulation in *section 1.4.1*, **different approaches for stimulation modulation were employed in previous studies. However, a direct comparison of the effectiveness of different**

encoding schemes to communicate feedback variables and facilitate myoelectric control is rarely conducted.

While above studies showed promising results in providing electrotactile feedback regarding the prosthesis' state, one common aspect in these studies was that EMG and stimulation electrodes were not placed together. Instead, stimulation electrodes were placed on the upper arm [100] or the contralateral arm [55], [67], [119], [120], or EMG was replaced by a joystick to control the prosthesis instead [57]. The reason for physically separating the stimulation from the recording is that the electrical pulses interfere with the recorded EMG. The strong stimulation artefacts impair the quality of control and thus compromises the prosthesis effectiveness and user experience.

1.4.3. ELECTRICAL ARTEFACT SUPPRESSION

The suppression of electrical pulses in EMG recordings has been an issue of interest also within the field of functional electrical stimulation (FES) [121]–[125] for rehabilitation of muscle activation in patients with a motor disability. Here the EMG signal (intention of movement) can be used as a trigger to deliver the FES. A particular objective of the signal processing is to remove the M-wave which is produced by the FES itself while extracting the volitionally produced EMG signal that reflects user motion intention.

When applying electrotactile stimulation for closed-loop myoelectric control, the stimulation is used to produce sensation and not to activate muscles. Thus, the artefact is of smaller amplitude. However, the EMG signal is recorded from multiple channels and is provided to a delicate control system that must accurately estimate user intention. The presence of stimulation pulses has shown to reduce the control accuracy dramatically when using neural networks [126] or linear discriminant analysis (LDA) [127] for pattern classification. Therefore, the noise in the EMG recording needs to be eliminated as much as possible for the movement patterns to be correctly discriminated. As mentioned, the stimulation and recording electrodes could be placed contralaterally [67], or spatially separated ipsilaterally [100], [128], where a distance of more than 6 cm has shown to limit the interference significantly [129]. However, such approaches would make the integration of the electrotactile interface into the socket more challenging. Only, few studies investigated simultaneous stimulation and recording without separating electrodes spatially by using time-division multiplexing [130] or artefact blanking [127]. In the former method, the stimulation was divided into on and off segments while the EMG signal was continuously acquired. The recording containing artefacts was discarded and only the artefact-free recording was used for myoelectric control. While providing stable control, the time-division multiplexing approach increases time delay in prosthesis response and disrupts the feedback flow. Artefact blanking, however, is a selective approach where the artifacts generated by individual pulses are suppressed, while the artefact-free EMG signal is retained. In pattern-recognition-based myoelectric control, the incoming EMG signal

is segmented into time-windows from which features are calculated and used as input to the control system. In [127], different strategies on how to handle blanked data intervals in time-windows for feature extraction were evaluated offline, showing no difference in classification accuracy when compared to an entirely artefact-free EMG signal. The advantage of the artefact blanking method is that it does not introduce time delay or disrupts the flow of feedback. **Translating the promising results from [127] into an online application would demonstrate a solution for closed-loop myoelectric control using electrotactile stimulation where recording and stimulation electrodes are placed next to each other. However, this challenge has not yet been addressed in the literature. Enabling simultaneous recording and stimulation would establish electrotactile stimulation as a practically applicable technology and motivate further exploration of electrotactile feedback in the scientific community.**

1.4.4. COMMUNICATION OF MULTIPLE FEEDBACK VARIABLES

Commercially available multifunctional myoelectric prostheses such as Bebionic Hand (Otto Bock, Duderstadt, Germany) [131] and iLimb (Össur, Reykjavik, Iceland) [132] contain actuation motors in individual fingers enabling various hand gestures. The Michelangelo Hand from Otto Bock [133] contains a single motor to drive the flexion and extension all four fingers and thumb with the possibility of attaching an active wrist [25]. In addition, force sensors are embedded in the Hand [133]. The flexion and rotation angle of the fingers and wrist, respectively, can be also read from the prosthesis sensors. Thus, three feedback variables (grasp force, hand aperture, and wrist rotation) need to be conveyed to communicate the full state of the prosthesis.

Only few previous studies communicated more than a single variable of a closed-loop myoelectric prosthesis through either invasive [63], [134]–[136] or non-invasive stimulation [61], [95], [99], [100]. Information on fingertip pressure and proprioception was provided through peripheral nerve stimulation by modulating the frequency of selected channels linearly [134], [135] and using intensity modulation [63], [136]. Vibrotactile stimulation was used to communicate grasp force and hand aperture through intensity and spatial modulation of a prosthesis placed remotely [99] and a virtual prosthesis controlled using a computer mouse [61], [95]. Spatial modulation of an array of vibration factors and amplitude modulation of an electrode grid placed on the upper arm transmitted information about finger joint angle and grasp force, respectively, of a prosthesis placed on a table [100]. Thus, the solutions proposed in the literature, so far, have conveyed at most two feedback variables, namely, grasp force and hand aperture. In general, as also indicated by the literature overview in *section 1.4.1* and *1.4.2*, **grasp force is most commonly investigated feedback variable, whereas the methods to convey the proprioceptive information about the prosthesis' state (hand aperture and wrist rotation) are less addressed in the literature.**

The studies using invasive stimulation methods do not compromise the feasibility of integrating the full closed-loop setup in a single system. However, as mentioned in *section 1.3.1*, the surgical intervention can be a hindrance amongst prosthesis users to apply invasive solutions. In the studies mentioned in the previous paragraph using superficial stimulation, the feedback was designed in a fashion that ignored the spatial limitation of a possible in-socket solution especially for users with proximal transradial amputations. For instance, in all cases, individual feedback variables were communicated by separate stimulation displays divided by notable distance. In [61], [95], [99], an array of vibration factors (first display) was placed circumferentially proximally on the forearm to communicate one feedback variable by spatial modulation, and a single larger factor (second display) was placed more distally to communicate the other feedback variable by amplitude modulation. In [100], an array of vibration factors (first display) was placed distally on the upper arm communicating hand aperture through spatial modulation, and an electrode grid (second display) was placed more proximally to communicate grasp force through amplitude modulation. The size of such stimulation setups would likely be too spacious to fit inside the prosthesis socket or be useful for users with proximal transradial amputations. Alternatively, the multiple feedback variables can be communicated by a single stimulation display, e.g., multichannel electrotactile array [116]. In [116], feedback encodings were designed to communicate the full state of a multifunctional prosthesis through a 16-channel electrode array by exploiting the high spatial and parameter resolution of the electrotactile display. Information regarding discrete intervals of hand aperture and wrist rotation angles were conveyed through spatial coding schemes, and the levels of grasp force were communicated by adjusting the stimulation frequency. However, the feedback was only evaluated psychometrically and only for each feedback variable independently. The high success rates indicated that subjects intuitively understood the individual feedback encodings, and the study provided inspiration on how to combine multiple feedback variables into a single encoding. **However, no study using non-invasive stimulation has yet directly evaluated the communication of multiple feedback variables using a single stimulation display during online closed-loop myoelectric prosthetic control tasks or communicated simultaneously more than two feedback variables (full state of prosthesis).**

Furthermore, in the previously mentioned studies communicating more than a single feedback variable using non-invasive stimulation, the subjects did not wear the prosthesis and equipment for closed-loop control on the ipsi-lateral forearm [61], [95], [99], [100]. In [99], [100], the prosthesis was placed on a table and in [61], [95] it was represented virtually. Thereby, the studies were disregarding the added weight from the prosthesis which can challenge the control robustness [137] and leaving out the incidental feedback produced by the prosthesis motors. By not mounting the full closed-loop setup on the same forearm, the improvement that the supplementary feedback might show to have on myoelectric control performance cannot be practically justified.

1.5. AIM OF THE PROJECT

The preceding chapter analyzed the state-of-the-art within closed-loop myoelectric control and highlighted unaddressed and/or scarcely investigated areas in the literature. These points are summarized below, and they motivated the aims of the present work.

The electrotactile technology allows multiple approaches to modulate the stimulation to represent feedback variables describing the prosthesis' state, namely, intensity, frequency, temporal and spatial modulation. Most studies have focused on communicating grasp force, despite prosthesis users expressed an interest to additionally receive the proprioceptive information (hand aperture and wrist rotation). **An aim of the PhD project was, therefore, to compare the effectiveness of different feedback encodings to communicate the proprioceptive information of the prosthesis' state and facilitate myoelectric control.**

Compared to vibrotactile feedback, electrotactile stimulation is less frequently applied in the literature to communicate sensory information in closed-loop myoelectric control. One reason for this is that when the stimulation and recording electrode are placed adjacently (inside the prosthesis socket) electrical pulses interfere with the myoelectric recording leading to unreliable prosthetic control. Blanking of the electrical artefact in the EMG recording has shown to be an effective technique to improve offline classification accuracy. **Therefore, an aim of the PhD project was to show the feasibility of using online artefact blanking for stable closed-loop myoelectric control with stimulation and recording electrodes placed adjacently on the ipsilateral forearm.**

Previous studies communicating more than a single feedback variable using non-invasive stimulation, did not consider the spatial confinement of an in-socket solution nor did the subjects wear a physical prosthesis. The information provided by the incidental feedback from the prosthesis was therefore not considered, and the developed supplementary feedback was not compared to the baseline (incidental feedback). Furthermore, no study has yet communicated simultaneously the full state (hand aperture, wrist rotation and grasp force) of a multifunctional prosthesis during online closed-loop control. **Therefore, the aims of the PhD project were 1) to enable that the entire closed-loop prosthetic setup is worn on the ipsilateral forearm, and 2) to compare the myoelectric control performance during a functional task when receiving supplementary feedback about the full state of the prosthesis versus when relying only on the incidental feedback (baseline performance).**

1.5.1. RESEARCH QUESTIONS

Merging the above stated aims, the grand objective of the present PhD project was to demonstrate a self-contained solution for closed-loop prosthesis control where electro-tactile stimulation is employed to effectively convey the full-state of a multifunctional prosthesis. Research questions were formulated to address the aims of the project:

- RQ1.** How can multiple feedback variables be communicated in a single feedback coding scheme using a single stimulation display to improve myoelectric control performance? Do the subjects find specific modulation of the stimulation more intuitive to understand than others?
- RQ2.** How can stable control be achieved while delivering electro-tactile feedback simultaneously with EMG recording and with stimulation and recording electrodes placed adjacently?
- RQ3.** Can the full state of a multifunctional myoelectric prosthesis be conveyed to the user in an intuitive manner that allows reliable perception and easy interpretation? What is the benefit of supplemental electro-tactile feedback compared to incidental feedback from the prosthesis?

Three studies were designed and completed in the effort of providing qualified answers to the posed research questions.

Study I: “Amplitude versus spatially modulated electro-tactile feedback for myoelectric control of two degrees of freedom” [1]

As an effort to address **RQ1**, Study I was designed. Novel feedback coding schemes based on amplitude and spatial modulation, respectively, were designed using a multichannel electrode array placed circumferentially around the forearm to communicate the proprioceptive information of hand aperture and wrist rotation. The novel spatial encoding resembled the movement of the wrist rotation and finger/thumb position during closing/opening of the hand. Stimulation on the dorsal side of the forearm moved in sync with the rotation of the prosthesis wrist and oppositely placed electrode pads on the volar side imitated the movement of the fingers and thumb when closing hand by decreasing the pad distance until the hand fully closed. In the novel amplitude-based scheme, wrist pronation, supination and hand aperture were represented by activating fixed pad groups, and an increase in either DoF was communicated by increasing the stimulation amplitude. As the aim was to directly compare the effectiveness of the two coding schemes through myoelectric control performance, the participants controlled a virtual prosthesis. The electro-tactile stimulation was applied to the contralateral forearm to avoid contaminating the myoelectric signal that would otherwise disrupt the control and mask the effectiveness of the feedback encodings.

Study II: “A compact system for simultaneous stimulation and recording for closed-loop myoelectric control” [2]

Study II was conducted to address **RQ2**. A novel device containing both electrotactile stimulation and EMG recording units allowed online blanking of electrical artefacts in the EMG recording. The device was used to show the feasibility of placing both recording and stimulation electrodes on the ipsilateral forearm while retaining stable control. A novel feedback scheme communicating wrist rotation and hand aperture through spatial and parameter modulation, respectively, was designed to provide useful feedback to the subjects while stressing the control by changing the length and frequency of blanked signal intervals. The myoelectric control performance was compared with and without electrotactile stimulation during control of a virtual prosthesis.

Study III: “Closed-Loop Control of a Multifunctional Myoelectric Prosthesis With Full-State Anatomically Congruent Electrotactile Feedback” [3]

Study III addressed **RQ3** but also addressed **RQ1** and **RQ2** by comparing different feedback encodings while using ipsilateral placement of recording and stimulation electrodes. A novel feedback encoding was designed to convey the full state of wrist rotation, hand aperture, and grasp force of a multifunctional prosthesis. The spatial motion of the wrist and fingers were coupled to communicate the proprioceptive information of the prosthesis in an anatomical congruent manner. Two electrode pads rotated synchronized with the direction of the prosthesis' wrist with a fixed inter-pad distance and the distance between the two pads changed as the hand began to close to follow the movement of the fingers and thumb. Grasping force was additionally conveyed through parameter modulation of the active electrode pads, effectively communicating three feedback variables simultaneously through a single stimulation display. The novel feedback coding was compared to the spatial encoding evaluated in Study I, in which wrist rotation and hand aperture feedback variables were sectorized on the dorsal and volar side of the forearm, respectively, and grasp force was similarly communicated using parameter modulation. Subjects wore the entire setup of recording and stimulation electrodes and physical prosthesis on the ipsilateral forearm, and the myoelectric control performance was compared when receiving the electrotactile feedback versus incidental feedback only (no visual feedback).

CHAPTER 2. EQUIPMENT

In all studies, EMG was used as signal source for prosthetic control, and electrotactile stimulation was used to provide feedback about the state of the prosthesis. In Study I, the EMG signal was recorded from the dominant forearm and the stimulation was delivered to the contralateral arm using separate devices, see *Fig. 2a*. In Study II, the recording and stimulation electrodes were placed on the same forearm and connected to the same device, see *Fig. 2b*. In Study III, the subjects additionally wore a physical prosthesis on the ipsilateral forearm as shown in *Fig. 2c*. These closed-loop myoelectric control components are described in the following sections. All interfacing with the equipment was conducted through a PC using MatLab (MathWorks, USA).

2.1. MYO ARMBAND

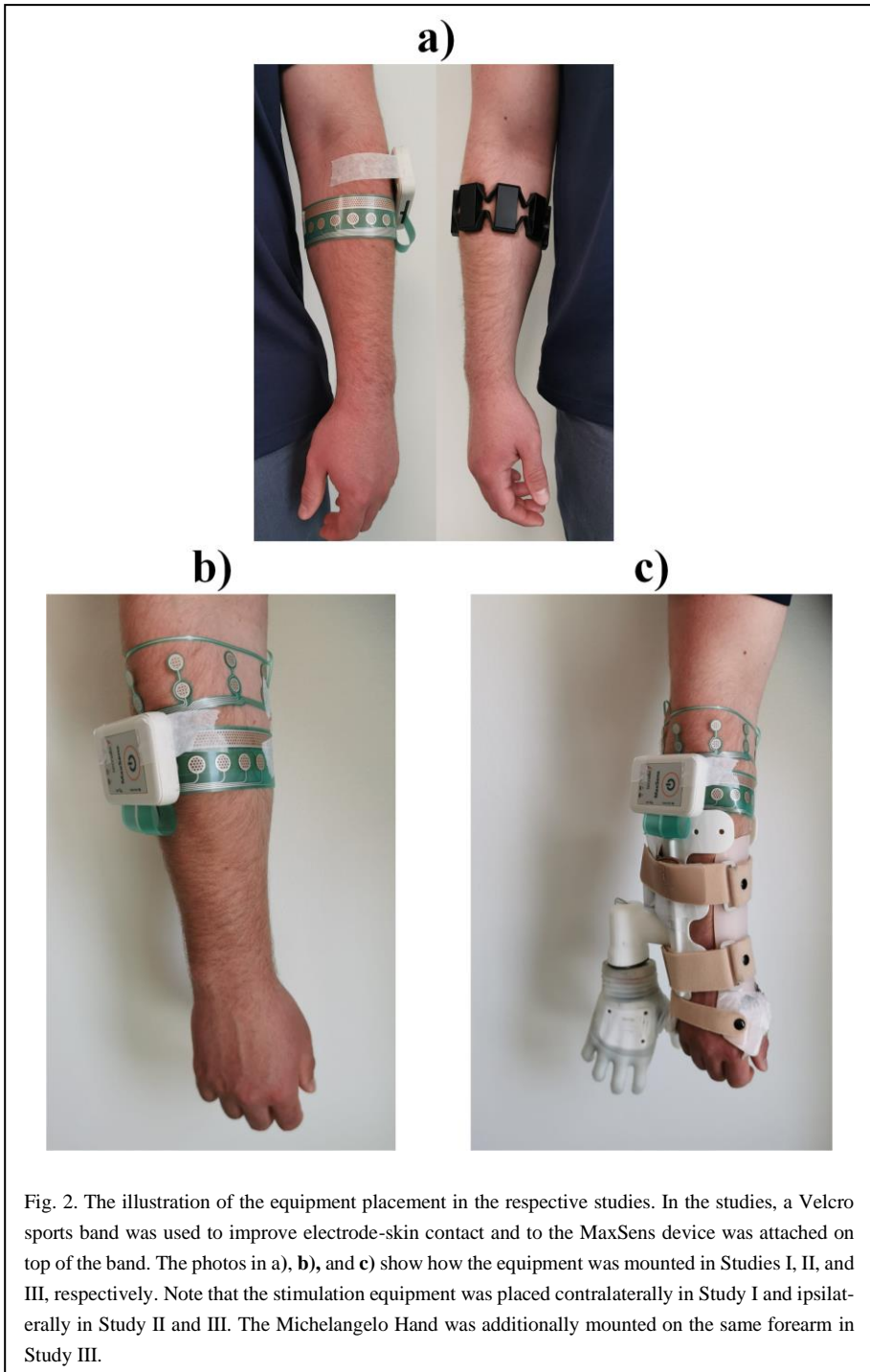
In Study I, the Myo armband developed by the Canadian company previously known as Thalmic Labs was used to record EMG signals, see *Fig. 3a*. The armband contains eight embedded bipolar stainless-steel electrode channels that are dry and do not require disposal after use. The armband is stretchable and can be further tightened with clips so that it can be adjusted to forearms of different thickness while ensuring equidistant spatial separation of channels. It communicates wirelessly via Bluetooth 4.0, eliminating the presence of wires that may restrict mobility. The sample rate of the armband is 200 Hz, and it contains an integrated 50-Hz notch filter for the removal of noise from the power grid.

2.2. MAXSENS DEVICE

In Study II and III, the EMG signal was recorded using the MaxSens device (Tecnalia Research & Development, Spain), see *Fig. 3a* [138], and the device was used in all studies to provide electrotactile stimulation. The device was developed in a collaborative effort before the inception of the PhD project. The hardware description of the device is documented in detail in the publication associated to Study II [2], but a summary of the components is provided in the following sections.

2.2.1. EMG RECORDING

The EMG signal can be acquired using either the eight circular pad-pairs (bipolar configuration) or single pads from the pad-pairs (monopolar configuration) and the three large reference pads, see *Fig. 3a*. The electrode pads consist of conductive Ag/AgCl traces embedded within a 150 μm polyester layer. To improve the electrode-skin contact, the pads were covered with conductive hydrogel (AG702, Axelgaard, Denmark). The electrode was printed in three different sizes to accommodate forearm thicknesses expected from healthy able-bodied subjects. The signal can be transmitted



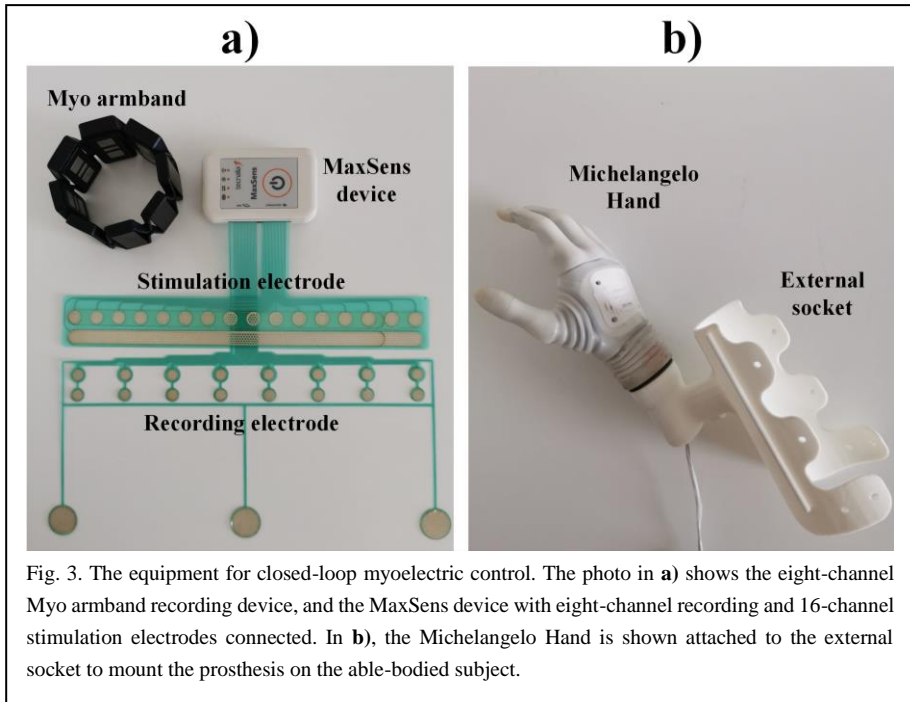


Fig. 3. The equipment for closed-loop myoelectric control. The photo in a) shows the eight-channel Myo armband recording device, and the MaxSens device with eight-channel recording and 16-channel stimulation electrodes connected. In b), the Michelangelo Hand is shown attached to the external socket to mount the prosthesis on the able-bodied subject.

both via USB cable and wireless Bluetooth connection. The sample rate can be set to 250, 500, 1000 or 2000 Hz, and the gain can be set to 1, 2, 4, 8, 12 or 24.

2.2.2. ELECTROTACTILE STIMULATION

The electrode array consisted of 16 active circular pads and an elongated reference pad [116] and was fabricated using the same material as the recording electrode. The pads were covered with the hydrogel to increase conductivity, see Fig. 3a. As for the recording electrode, three sizes were produced to accommodate varying forearm thicknesses in the subjects. The MaxSens delivered asynchronous rectangular bi-phasic pulses. The pulse amplitude and width could be adjusted for individual pads in the range of 10-500 μ s in increments of 10 μ s and 0.1-10 mA in increments of 0.1 mA, respectively. The pulse frequency was a common parameter for all pads and could be modulated in the range of 1-400 Hz in increments of 1 Hz.

2.2.3. STIMULATION ARTEFACT BLANKING

The MaxSens device contains both recording and stimulation units with bidirectional communication and precise synchronization that allows for blanking of stimulation pulses in the EMG recording (see Fig. 4 for artefact influence when blanking is off and on). A sample-and-hold technique is used, such that when stimulation is produced,

the value of the last recorded sample is copied to the subsequent samples until the blanking interval is finished (see *Fig. 5a*). The number of blanked samples for one stimulation pulse is determined based on the pulse width, amplitude, and number of active pads [2], where the higher those parameter are, the more samples are blanked. Specifically, when more pads are activated, the pulse generated from each pad is delivered asynchronously separated by an inter-pulse interval. Thus, in case that all pulses have the same duration, the blanking duration is proportional to the sum of the pulse width and inter-pulse interval times the number of active pads. However, as the skin acts as a capacitor, the blanking duration was prolonged further by an experimentally derived function of pulse width and amplitude, see Equation 1 in [2]. The

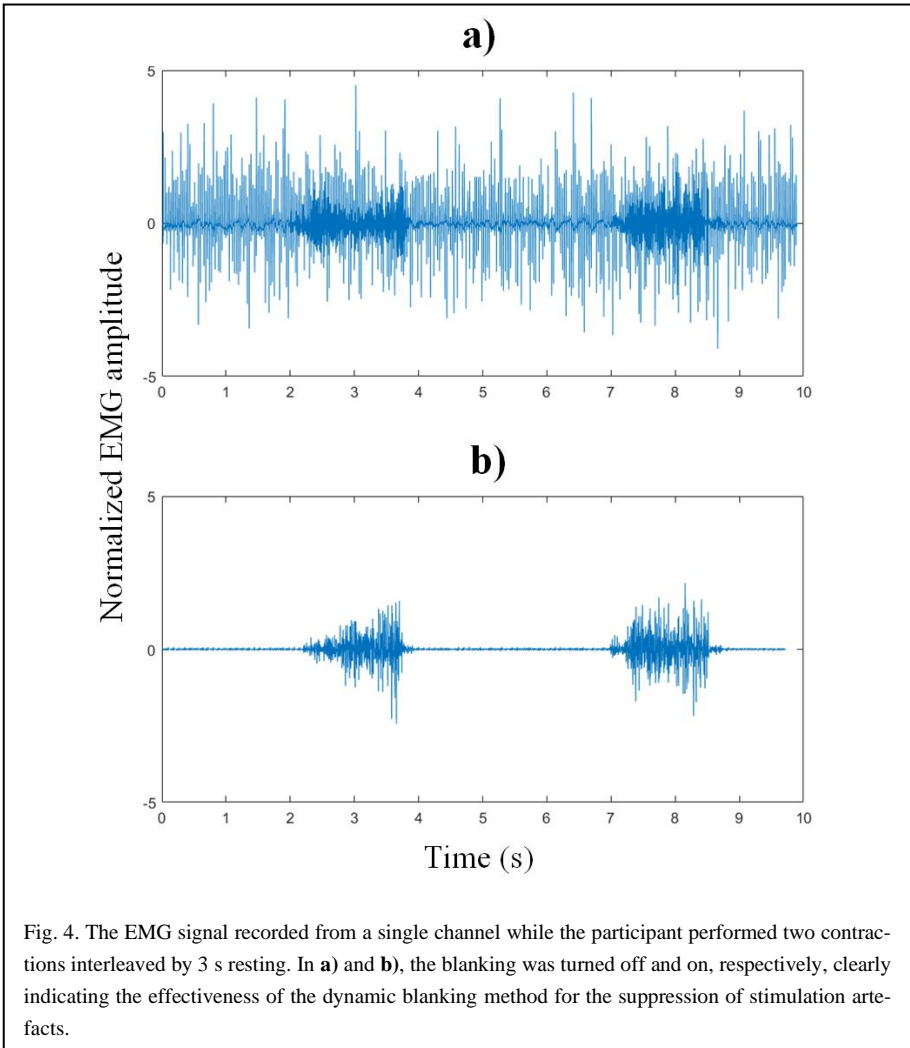


Fig. 4. The EMG signal recorded from a single channel while the participant performed two contractions interleaved by 3 s resting. In **a)** and **b)**, the blanking was turned off and on, respectively, clearly indicating the effectiveness of the dynamic blanking method for the suppression of stimulation artefacts.

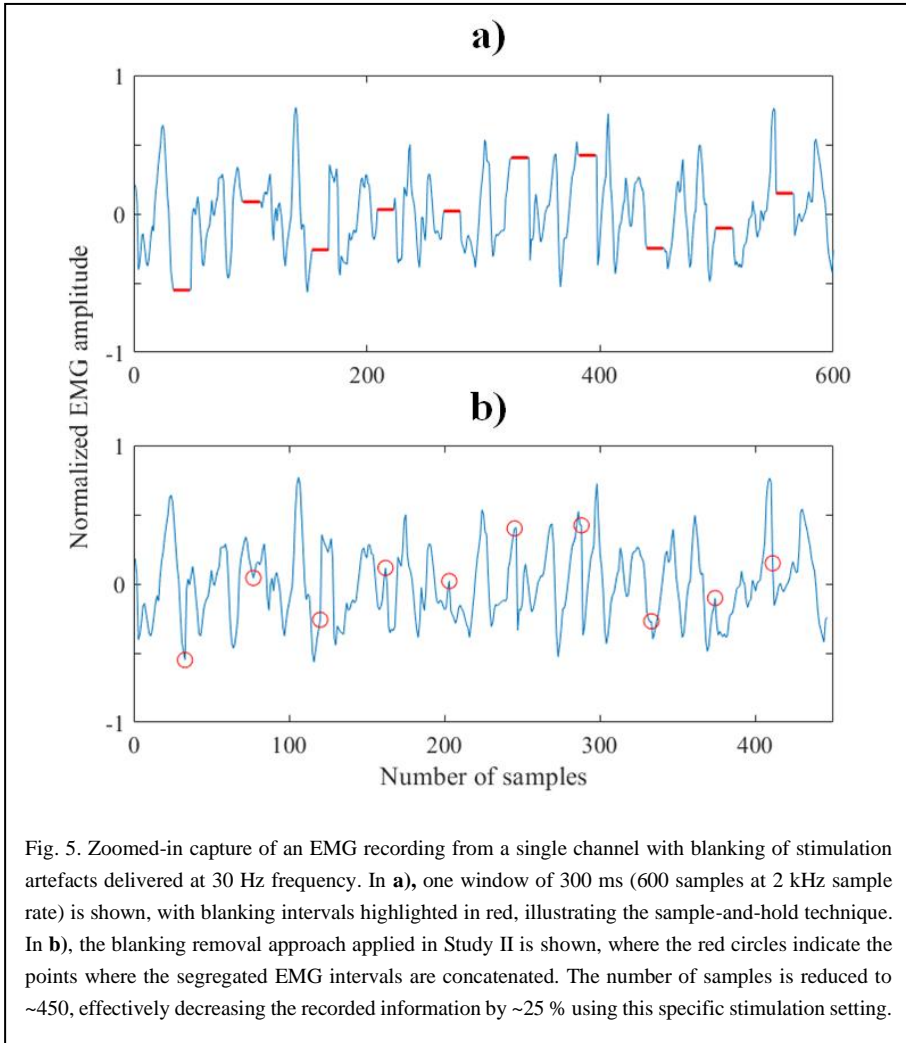


Fig. 5. Zoomed-in capture of an EMG recording from a single channel with blanking of stimulation artefacts delivered at 30 Hz frequency. In **a)**, one window of 300 ms (600 samples at 2 kHz sample rate) is shown, with blanking intervals highlighted in red, illustrating the sample-and-hold technique. In **b)**, the blanking removal approach applied in Study II is shown, where the red circles indicate the points where the segregated EMG intervals are concatenated. The number of samples is reduced to ~450, effectively decreasing the recorded information by ~25 % using this specific stimulation setting.

stimulation frequency determined the occurrence of blanking intervals, where an increase in frequency introduced more blanking intervals into the recording.

2.3. MICHELANGELO HAND

In Study III, the subjects controlled a physical prosthesis, the multifunctional Michelangelo Hand [133] and wore it using an external socket seen in *Fig. 3b*. The hand can move in two DoFs, hand opening/closing and wrist rotation. As mentioned in *section 1.4.4*, the hand contains a single motor to flex all fingers and the thumb simultaneously, where the thumb can be separately actuated to perform two grasp types (palmar and lateral). However, only palmar grasp was utilized in the present project. The hand

aperture range in palmar grasp is ~11 cm to 0 cm with a maximum velocity of ~0.4 s and the grasp force in the range of 0-70 N. The range of motion for the wrist rotation is from 160° to 160° with a maximum velocity of 25 rpm (full rotation ~3 s). Through Bluetooth communication, the rotation, aperture, and force levels can be read from the sensors embedded in the prosthesis as normalized values in the range of -100 to 100, 0-100, and 0-100, respectively. Thus, the aperture DoF is represented by half the number of values compared to the rotation DoF, and the neutral positions of 0 correspond to the hand fully open for hand aperture and midway of the rotation extremes in each direction for wrist rotation (wrist horizontal). Movement commands are transmitted from the host PC to the prosthesis through the Bluetooth connection.

CHAPTER 3. MYOELECTRIC PROSTHETIC CONTROL

In this chapter, the implementation of the myoelectric control is described. Initially, an overview of the procedures necessary for enabling myoelectric control is provided, after which the specific implementation for each procedure is explained.

3.1. MYOELECTRIC CONTROL USING PATTERN RECOGNITION

The control system of a pattern recognition-based myoelectric prosthesis uses a machine learning algorithm to generate a movement output. As EMG is a stochastic signal that varies largely between individuals, the control system needs to be calibrated for individual users specifically, and also after each donning on and off in the same user as the skin electrode interface changes (electrode positioning, skin properties etc.) [139]–[141]. Before the user can control the prosthesis in real-time/online, the control system needs to be modelled to accurately recognize and differentiate EMG patterns related to the performed hand movements, also referred to as training the control system.

The EMG signal can be acquired from electrodes placed on the surface of the skin or by using intramuscular electrodes that can collect individual motor unit action potentials. While intramuscular recordings provide information from an individual muscle and a less noisy signal, surface EMG is most commonly applied due to the ease of use. Typically, the EMG is recorded from an electrode array placed circumferentially around the forearm with multiple recording points arranged equidistantly [142]–[144]. EMG is acquired using either mono- or bi-polar configuration. The former method measures the electrical potential between active electrode pads placed on the skin above muscles and a reference pad placed on a neutral site (condyles of the bone), where the latter measures the electrical potential between electrode pad-pairs both placed on the skin above muscles. Monopolar recordings are prone to containing common noise across the multiple channel recordings due the common reference point [145]. In all cases, the active electrodes should be placed on the bulkiest section of the muscle to ensure optimal signal quality [22]. To ensure a low skin-electrode impedance and more stable contact, the skin can be prepared before electrode placement [146], [147]. The EMG signal is typically preprocessed by an analogue filter (usually a 50 Hz notch and anti-aliasing filter) before it is sampled through an analogue-digital converter. As the EMG spectrum is in the range of approximately 10-500 Hz, a sample rate of at least 1000 Hz is recommended to avoid aliasing and retain the signal frequency content [23], [148]. The analogue components described so far comprise the recording equipment.

On the digital side of the pattern classification pipeline, further signal processing can be performed, e.g., filtering, artefact removal etc., before segmenting the signal into temporal windows (data segmentation). During online control, the temporal length of the window is a compromise between control accuracy (longer windows give more temporal context) and delay (shorter windows enable control output at a faster rate). Overlapping between consecutive windows is often employed to capture temporal continuity and ensure a smooth transition. 150-250 ms windows with 50 % overlap is recommended as an appropriate trade-off between accuracy and delay [149]. Features describing the amplitude and frequency content are calculated from the samples contained in each window to extract relevant information from the signal (feature extraction). Typically, the features are calculated directly in the time-domain due the faster computation compared to transforming the signal to the frequency-domain [150]. To record the data to train the classifier, the subject is asked to perform desired hand movements while the EMG is acquired (training data acquisition). The EMG signal changes characteristics at different contraction intensities and at various states of the contraction: transient (increase and decrease of muscle force) and steady state (stable contraction) [23], [151]. To create a control system that can capture these changes in the signal, transient and steady state of the EMG should be included in the data acquisition [151], [152]. The features extracted from the training data are used to fit a pattern recognition model. When using a sequential control system, the features and associated movement labels are used as training data for a single classification model. A proportional control model that estimates the intended prosthesis movement velocity based on the EMG amplitude needs to be added as an extra component, as the classifier only determines the intended movement class. Regression models trained for each hand movement can be used to determine the proportional output. A simple but commonly used approach is to estimate the total muscle activation level by computing the average mean absolute value or root mean square of the windowed EMG signal across all channels. This value is then normalized to the EMG amplitude recorded when the subject performs the maximum voluntary contraction (MVC) and mapped to the normalized prosthesis command input (i.e., EMG of 1 leads to prosthesis closing at the maximum velocity during closing and produces maximum grasping force after contact). When using a simultaneous control system, the regression models can be used directly to decide both movement and proportional control output, by selecting the highest output value of the models from each DoF. Finally, the trained control system is ready to evaluate incoming EMG signals to estimate an online control output that is mapped into a prosthesis action (output mapping).

3.2. RECORDING EQUIPMENT

The Myo armband used in Study I samples the EMG signal at 200 Hz and does not have an anti-aliasing filter integrated. Thus, the signal frequencies above 100 Hz are aliased. Nevertheless, offline analysis using an LDA classifier demonstrated that using the armband can achieve comparable accuracy to conventional gel electrodes sampling at 1000 Hz [153], and the armband has also been frequently applied for pattern

recognition in myoelectric prosthetic control [154]. The armband was placed on the thickest part of the forearm to cover as many muscles as possible to facilitate the recognition of different hand gestures.

In both Study II and III, that used the MaxSens for EMG recording, the bipolar recording configuration was used. Less of common noise signal was captured from each channel compared to the monopolar setting, thereby facilitating greater discriminability of hand movements. The electrode size that each subject applied was selected so that the distance between the two extreme pad-pairs meeting on the volar side of the forearm was as similar as possible to the distance between the other neighboring electrode pairs. As with the Myo armband, the electrode was placed on the thickest part of the forearm. To ensure that pads were in stable contact with the skin, a Velcro sport band was used to tighten the fit, and the MaxSens device was then placed on the top of the band. In Study II, the USB connection was used but this was changed to wireless connection in Study III to demonstrate the feasibility of a mobile wearable solution. The sample rate was fixed to 1 and 2 kHz in Study II and III, respectively, for accurate signal representation (no aliasing). The sample rate was reduced between the two studies as the data transmission using Bluetooth was more stable at a lower sampling frequency especially when the wireless Bluetooth interfacing with the physical prosthesis was additionally included in the loop.

3.3. DATA SEGMENTATION

In Study I, a window length of 200 ms with 100 ms overlap was implemented, effectively computing the control decision every 100 ms using 200 ms of EMG information [149]. During the 100 ms window, the signal was acquired, processed and stimulation commands were transmitted to the MaxSens device. Pilot tests showed that the 100 ms update frequency was the minimum duration required to perform the required to complete both the control and stimulation pipeline. In Study II, the window length was further increased to 300 ms with an overlap of 100 ms, updating the control output every 200 ms using 300 ms EMG information. The update frequency was decreased to accommodate more complex processing due to increased sampling rate (more data) and additional processing steps (see next *section 3.4*). However, pilot tests indicated that the 200 ms update frequency did not affect the performance and user experience. In Study III, the window size was decreased from 300 ms to 200 ms (with no overlap) to reduce the amount of data while retaining the update frequency. This was required to accommodate the more complex signal processing (as in Study II) and an additional communication and processing loop due to interfacing with the physical prosthesis.

3.4. SIGNAL PROCESSING

Digital filtering of the acquired EMG signal was implemented in all studies. A 2nd order Butterworth high-pass filter with cut-off frequency at 15 Hz was applied for

removal of motion artefacts. In Study I, an analogue 50-Hz notch filter was already integrated in the Myo armband and the low 200 Hz sample rate caused aliasing leaving no need for a digital lowpass filter. No further signal processing was needed to denoise the acquired EMG signal in Study I. In Study II and III, a 50-Hz notch filter and a 2nd order Butterworth lowpass filter with the cut-off at 350 Hz were implemented.

In Study II, the recording was performed simultaneously with stimulation and the EMG signal was exposed to blanking. The blanking intervals were therefore identified, removed and the segregated signal parts were concatenated (see *Fig. 5b*) as recommended in [127]. As shown in [127] the removal of blanked intervals resulted in a significantly higher classification accuracy compared to retaining the blanked intervals. Another approach for similarly accurate control would have been to wait for enough non-blanked samples to arrive to replace the removed blanked samples, effectively increasing the window length [127]. The former approach was implemented to retain the window length of 300 ms and avoid output delay.

In both Study II and III, the adjacent placement of recording and stimulation electrodes demanded more elaborate processing of the recorded EMG signal when the electrotactile stimulation was active during online control. In both studies, the occurrence of outlier samples with large amplitude was observed (see *Fig. 6a*). Therefore, a sliding 10-sample Hampel outlier-removal filter was applied. For each sample, the median of the 10 neighboring samples (five on each side) was computed, and the same samples were used to calculate the median absolute difference. If the sample was more than three times higher than the median absolute difference, the sample was replaced with the median.

For Study III, the stimulation introduced further artefacts, perhaps due instability in the internal unit communication and data transmission when using the Bluetooth connection despite reducing the sample rate from 2 to 1 kHz. Changing the activation of pads caused a signal offset in two recording channels (see *Fig. 6b* for an example), and the pilot tests showed that this caused unstable closed-loop control. To eliminate the offset, first the difference between consecutive samples (differenced EMG signal) was calculated for one window to accentuate the offset. The standard deviation of the differenced EMG signal was computed and values higher than four times the standard deviation was set to zero, which reliably removed the offset while preserving signal amplitude information. As observed in [2], the blanking algorithm did not suppress the stimulation artifact completely introducing a small amplitude leakage after each blank (see *Fig. 6c*). Therefore, contrary to what was proposed in [127], the blanked stimulation pulses were not discarded from the signal. Instead, a comb and notch filter at the present and half the present stimulation frequency, respectively, were applied

to attenuate the leakage amplitude and its harmonics (see *Fig. 6*, for an example of a more severe case of the current leakage).

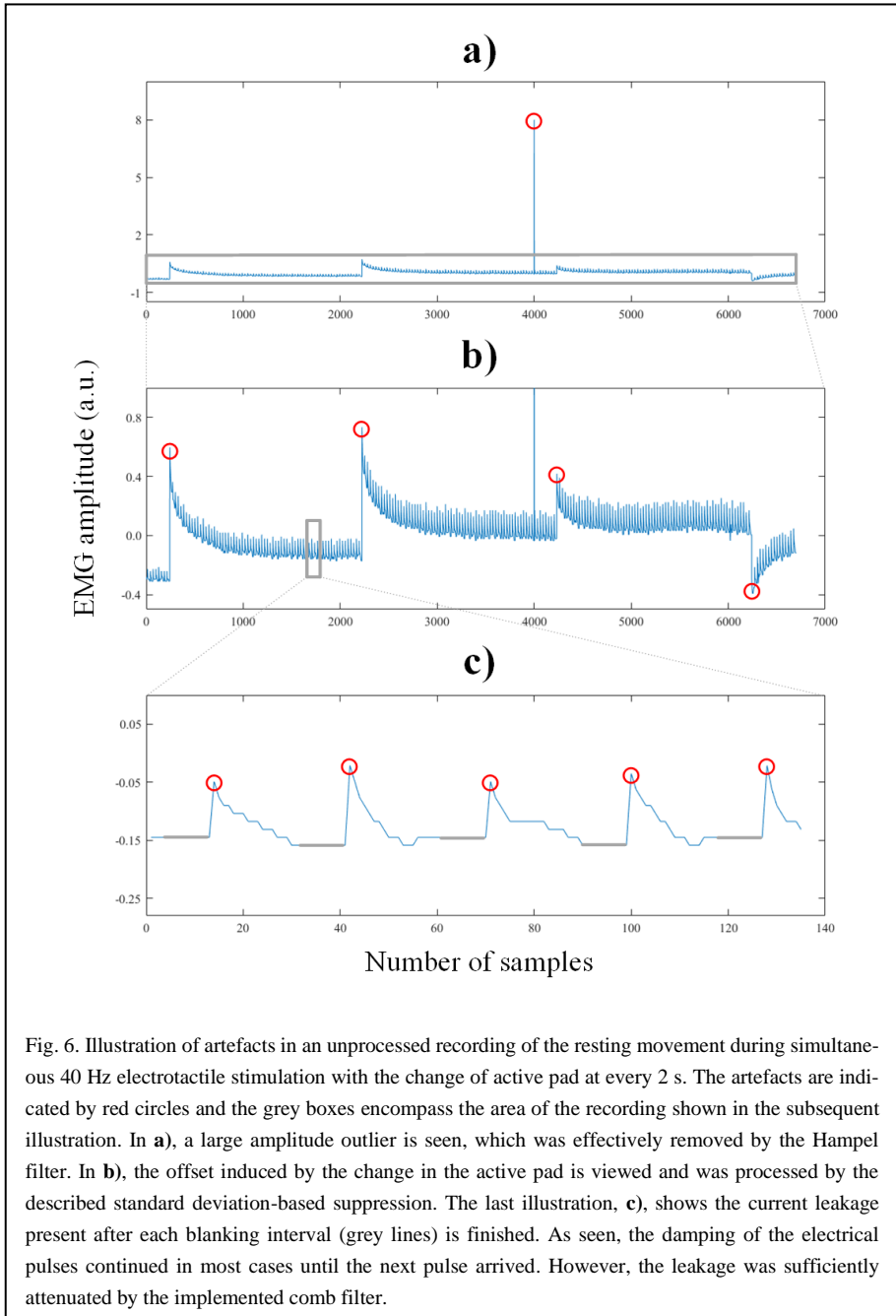


Fig. 6. Illustration of artefacts in an unprocessed recording of the resting movement during simultaneous 40 Hz electrocutaneous stimulation with the change of active pad at every 2 s. The artefacts are indicated by red circles and the grey boxes encompass the area of the recording shown in the subsequent illustration. In **a)**, a large amplitude outlier is seen, which was effectively removed by the Hampel filter. In **b)**, the offset induced by the change in the active pad is viewed and was processed by the described standard deviation-based suppression. The last illustration, **c)**, shows the current leakage present after each blanking interval (grey lines) is finished. As seen, the damping of the electrical pulses continued in most cases until the next pulse arrived. However, the leakage was sufficiently attenuated by the implemented comb filter.

3.5. FEATURE EXTRACTION

Traditionally, the benchmark time-domain features mean absolute value (MAV), waveform length (WL), zero crossings (ZC), and slope-sign changes (SSC) are extracted from the data windows [155], also referred to as Hudgins features. MAV is similar to the root-mean-square value and characterizes the intensity of muscle activation, WL describes both intensity and frequency content, and ZC and SSC are frequency content descriptors. The low sample rate in Myo armband aliases the frequency content of the signal and thereby also the information contained in the ZC and SSC features. In [156], an alternative set of features were proposed when using the Myo armband, characterizing the amplitude relationship between neighboring channels (i.e., space-domain features). Compared to Hudgins features, the space-domain features showed an increase in classification accuracy in an offline analysis. The space-domain features were therefore used in Study I. In Study II, the sample rate was appropriate, to preserve the frequency content of the recorded EMG and Hudgins features were therefore extracted. In Study III, regression was used for simultaneous control, and as usually done in the literature [30], [31], only MAV was extracted and used as input for the regressor.

3.6. TRAINING DATA ACQUISITION

Features were extracted from the EMG signals recorded in the training data acquisition. The strategy for data acquisition was similar across all three studies. EMG signals were recorded from active hand movements including wrist supination and pronation (wrist rotation DoF) and hand closing and opening (hand aperture DoF), along with the resting (no contraction). The MAV of the EMG signal was computed for each channel and averaged to estimate the overall level of muscle activation. This level was then represented as a cursor on a computer monitor, which moved horizontally with time and vertically with EMG amplitude. Initially, a 15-s baseline of rest was recorded along with the 15-s prolonged MVC (pMVC) of each active movement. These minimum and maximum EMG signal amplitude recordings were used to normalize the cursor movement (EMG amplitude) such that the lower and upper limit of vertical excursion corresponded to the baseline and pMVC recording, respectively. When acquiring the data used for feature extraction and training of the control system, the subjects were asked to trace a trapezoidal trajectory comprising a 3-second incline and decline, and an in-between 5-second plateau to capture transient and steady state of the muscle contraction, respectively [157]. Three recordings were acquired from each of the active movements, respectively, and the plateau was scaled to 40 %, 50 %, and 70 % of the pMVC. Lastly, a 15-s recording of rest was acquired.

In Study II and III, the baseline recording showed a higher amplitude during electro-tactile stimulation despite the implementation of firmware blanking and more elabo-

rate signal processing. Therefore, electrical stimulation was activated during the recording of the resting movement in an effort to increase control stability during rest. In Study II, eight electrode pads were simultaneously activated throughout the 15-s recording in the pattern of two active adjacent pads interleaved by two inactive adjacent pads. Stimulation parameter settings were 500 μ s pulse width, 50 Hz frequency and amplitude values calibrated at sensation threshold. In Study III, a sweep through the neighboring pad-pairs (2-s activation per pad-pair) was applied to better capture the spatial contamination from the coding schemes. Stimulation parameters settings were 400 μ s pulse width, 35 Hz frequency and amplitude values calibrated at localization threshold [158]).

In Study I and II, the training data was recorded while the subject was seated comfortable in a chair with the arm relaxed next to the body. In Study III, the subject performed a functional evaluation task with varying limb position. To account for the induced limb position effect, the training data were recorded with the subject standing and the elbow flexed to approximately 60° [31], [139].

3.7. PATTERN RECOGNITION AND PROPORTIONAL CONTROL

In Study I and II, the extracted features were used to train an LDA classifier and proportional control model to identify the movement intention and prosthesis velocity and force, respectively. This is a commonly applied combination for sequential myoelectric prosthetic control [27], [159]–[162]. In the training of the LDA classifier, the feature set of each hand movement class is modeled using a Gaussian distribution, by assuming that the classes share common co-variance matrix. Using this assumption, the posterior probability of each movement class can be calculated from the Bayes' rule, where the movement class with the highest probability is the output of the classifier (recognized motion). For proportional control, a separate multiple linear regression model was trained for each movement class to determine the intended movement velocity during closing and grasping force after contact. The input was the MAV of the EMG signal, and the output was set as the normalized MAV scaled from 0-1 with the pMVC as the upper limit. The target output for the rest class was set to zero when fitting regression, to induce greater stability when no movement was produced.

In Study III, multiple linear regression models, one per movement class, were trained and applied to estimate both movement intention and velocity for simultaneous proportional control. To enable simultaneous control, the output of the control system during online control was the highest value of the two regressors estimating wrist rotation (pronation/supination regressor) and hand aperture DoF (opening and closing regressor), respectively. While using regression models allows simultaneous movements, it can be prone to cross talk from the other DoF when wanting to perform single DoF motion. Therefore, the training of regression models was similar to that used in Study I and II to estimate the proportional activation after classification, but for each

movement class, the MAV of the EMG signal of the remaining movement classes were additionally included as input while the desired output was set to zero. To further increase stable one-DoF movement in Study III and increase control stability during resting in all studies, no proportional control output was produced when the contraction level was below 20 % of the pMVC of the recognized movement.

CHAPTER 4. ELECTROTACTILE STIMULATION TO COMMUNICATE SOMATOSENSORY FEEDBACK

This chapter describes the motivation and implementation of the novel feedback coding schemes designed to communicate proprioceptive information and grasping force. In all coding schemes the range of each feedback variable was discretized into distinct levels. While discretization of sensory feedback is not natural (as the natural feedback is continuous), it was selected as it allows the subject to interpret the feedback easily with minimal training. From discrete feedback it is also expected that the user can "interpolate" the levels to expand the information contained by the explicit feedback.

Common for all schemes was that no stimulation was provided when the prosthesis was in the neutral position of hand fully opened and wrist horizontal, which acted as a distinct point of reference. The schemes are described by assuming that they have been applied to a right-handed subject. The spatial information describing wrist rotation was mirrored for left-handed subjects. Before explaining the feedback encodings more in detail, the method for calibrating the stimulation intensity is initially described.

4.1. STIMULATION INTENSITY CALIBRATION

As mentioned in *section 1.4.2*, the intensity of the stimulation needs to be calibrated before use to ensure a comfortable sensation. Initially, the electrode array was placed on the forearm, where the size used by the individual subject was selected to approximating same distance between the extreme pads converging on the volar side of the forearm as for the remaining pads. Ensuring an equidistant pad separation was important for the spatial modulation to be perceived as envisioned.

In both Study I and II, the intensity was calibrated by determining both the sensation and discomfort thresholds, whereas in Study III, the localization threshold (clear and localized sensation) [158] was determined. The localization threshold was determined for Study III instead of the sensation threshold after subjects reported in Study I and II that the sensation threshold could be difficult to recognize especially when simultaneously controlling the prosthesis. In all studies, the ascending method of limits was applied to measure the thresholds. The pulse width and frequency were fixed at 500 μs (400 μs for Study III) and 50 Hz (35 Hz for Study III), and the amplitude was increased in steps of 0.1 mA starting from 0.5 mA. The subject reported when they felt the sensation (sensation threshold), the sensation was clear and still localized be-

low the pad (localization threshold) or the sensation became uncomfortable (discomfort threshold). To ensure homogenous sensation intensity across pads for the given sensation, discomfort and localization thresholds, the amplitude was subsequently adjusted by comparing the intensity of neighboring pads and increasing or decreasing the amplitude if needed.

4.2. SPATIAL VERSUS AMPLITUDE MODULATION

Aim

In Study I, the motivation was to compare different encoding schemes to communicate the same two DoFs of wrist rotation and hand aperture. The electrotactile feedback technology provides several possibilities for modulating the stimulation (e.g., many stimulation channels and large parameter range), however, the different encoding strategies were rarely directly compared in the literature. Thus, it has not yet been clearly defined whether one feedback modulation is more effective than the other. For this purpose, two novel feedback coding schemes were designed based on spatial and amplitude modulation, respectively, as these are two very different strategies to convey feedback information. The concept of the novel spatial encoding was that the stimulation produced moving sensations mimicking the natural motion of the prosthesis' wrist and fingers (see *Fig. 7a*). In the novel amplitude encoding, groups of pads were dedicated to representing wrist pronation, supination, and hand aperture, where the modulation of stimulation amplitude indicated different levels of the feedback variables (see *Fig. 7a*). In both schemes, each DoF was divided into five discrete levels.

Description of feedback schemes

For the spatial encoding seen in *Fig. 7a*, the array electrode was sectorized such that the rotation and aperture DoFs were conveyed by the eight pads on the dorsal and volar side, respectively. Two pads were activated to indicate the current level of each DoF, respectively. Therefore, either zero, two or four pads could be simultaneously active to communicate neutral, single, or combined DoF positions, respectively. The sector of the electrode assigned to wrist rotation was divided into two groups of pads on the dorsal side of the forearm, where the medial and lateral pad group indicated pronation and supination orientation, respectively. The pads were activated in pairs, as explained before, and the pad-pairs were activated sequentially to produce a sensation that moved counterclockwise across the forearm for pronation and clockwise for supination in two levels each, making a total of five levels when including the neutral wrist position. To convey hand aperture, two oppositely located pads (one on the medial and lateral side, respectively) were activated simultaneously. Such pad-pairs were then activated sequentially to produce sensations converging toward the volar side of the forearm. Therefore, the distance between the two sensations decreased as the hand was closing, resembling the fingers and the thumb coming closer together (and vice versa for the opening). The aperture DoF was also divided into five levels: one level for neutral position and four levels of closing.

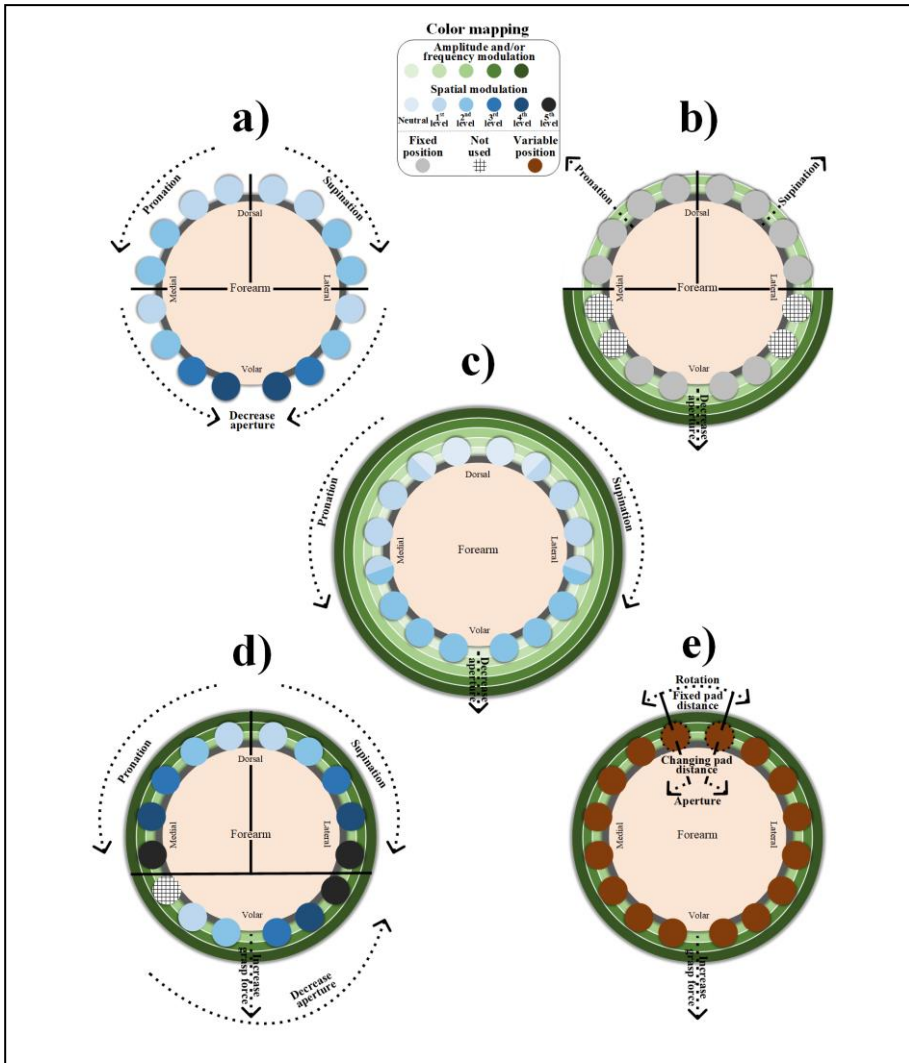


Fig. 7. The illustrations of feedback encoding schemes used in the studies. In **a)** and **b)**, the amplitude and spatial modulation scheme used in Study I are shown, respectively. The mixed amplitude and spatial coding scheme shown in **c)** was used in Study II and **d)** and **e)** illustrate the sectorized and coupled coding schemes used in Study III, respectively. The color coding indicates how the stimulation was modulated (see color mapping box in the top), while the arrows indicate the feedback variable that was communicated (rotation, aperture, or force). The “neutral” means either that the hand was fully opened (aperture DoF) or that the wrist was in the neutral horizontal position (rotation DoF) and was only actively conveyed in **c)**. Also, in **c)**, some pads overlap in feedback levels as spatial modulation of four pads indicated five levels and was divided between 16 stimulation pads. The white gridded pads in **b)** and **d)** were not used. The red color of the pads in **e)** indicates that the activation of the pads communicated multiple and variable information.

In the amplitude modulated scheme, the electrode was divided into sections to represent each DoF similarly to the spatial scheme. Groups of four neighboring pads represented wrist rotation (medial side for pronation and lateral side for supination) and hand aperture, respectively, see grey pads in *Fig. 7b*. So, either zero, four or eight pads could be simultaneously activated to convey neutral, single, or combined DoF positions, respectively. Four pads were used per section to exploit the capacity of the electrode array and produce clearer sensations (larger area of the skin). Pronation and supination were communicated using two amplitude levels for each movement (four levels for rotation) and the same approach was used for hand aperture, a total of five level per each DoF when including neutral position. To deliver discriminable amplitude levels, the sensation and discomfort thresholds were used as the first and last level. The intermediate second and third levels were represented using the amplitude values that equidistantly separated the four levels. The stimulation intensity corresponding to the second level in the amplitude scheme was applied to all pads in the spatial scheme.

4.3. MIXED ENCODING

Aim

The intention of the novel feedback encoding in Study II (see *Fig. 7c*) was to provide useful information by applying the intuitive concepts evaluated in Study I, but also to challenge the robustness of the control system by dynamically varying the duration and frequency of blanks along with the location of stimulation. Specifically, increasing the amplitude and frequency would prolong the blanking interval and rate of occurrence, respectively, and thereby result in less of the useful EMG information during the recording. In addition, spatial modulation of stimulation would induce artifacts in different recording channels (those closest to the stimulation location), and thereby possibly alter the recorded signal patterns and “confuse” the classifier. The idea was therefore to combine these methods and devise feedback encoding that would introduce maximum possible interference to the EMG control system due to the concurrent electrotactile stimulation.

Description of feedback scheme

The mixed encoding scheme designed to communicate wrist rotation and hand aperture is visualized in *Fig. 7c*. Similar to Study I, the ranges of both DoFs were discretized into five levels each. Wrist rotation was conveyed by employing the same concept as in the spatial modulation scheme of Study I, however, utilizing all 16 pads for the DoF. Therefore, groups of four neighboring pads were activated sequentially producing the sensation that rotated around the forearm mimicking the direction of the prosthesis wrist rotation, similar to spatial encoding of Study I. As 16 pads were divided into five levels, the activation of some pads overlapped between adjacent feedback levels as seen in *Fig. 7c*. Hand aperture was communicated by modulating simultaneously the stimulation amplitude and frequency of the four active pads. The five amplitude levels (neutral to fourth level) were determined as in Study I, except that

three (instead of two) intermediated levels were required. The frequency levels indicating the hand aperture were changed from 10 Hz in neutral position to 50 Hz for the fourth level (hand closed) with an increment of 10 Hz for intermediate levels.

4.4. COMMUNICATING FULL STATE OF PROSTHE-SIS

Aim

It is already well known that the motors in a multifunctional prosthesis provide incidental feedback regarding the prosthesis state. For instance, the motors driving the finger flexion and wrist rotation create discriminable vibratory and auditory cues indicating the active DoF(s) and increasing the velocity of movement increases the intensity of the cues. Similarly, as the grasping force increases, the finger flexion motors create discrete sound and vibratory bursts. In the literature, when evaluating the effect of adding supplementary feedback, such feedback is rarely compared to the feedback already provided by the incidental cues. Therefore, in Study III, the motivation was to evaluate whether supplementary feedback explicitly communicating the full state of a multifunctional prosthesis could effectively increase myoelectric control performance during a functional task compared to only receiving incidental feedback cues produced by the prosthesis (no visual feedback). Two electrotactile feedback coding schemes were designed, where one was similar to the spatial feedback scheme evaluated in Study I, in which the proprioceptive DoFs were communicated along the sectors of the forearm (see *Fig. 7d*). The other feedback encoding was a novel approach that coupled the movement of the stimulation representing the two DoFs to mimicking the movement of the wrist and fingers of the prosthesis, hence providing anatomically congruent sensations (see *Fig. 7e*). The second aim was therefore to compare the novel coupled feedback encoding to the “conventional” (previously validated) sectorized approach. The DoF ranges were divided into more levels compared to Study I and II (eleven and six levels for rotation and aperture, respectively) to maximally exploit the spatial capacity of the electrode array. The number of levels reflected the range of motion in each DoF (the motion range of rotation was twice that of aperture, recall *section 2.3*).

Description of feedback schemes

In the first encoding depicted in *Fig. 7d*, the electrode array was sectorized in a similar fashion as in *Fig. 7a* and is hereafter referred to as the sectorized coding scheme. The ten dorsally placed pads were dedicated to rotation, while five pads placed on the volar side of the forearm provided hand aperture information. One active pad represented the current level of rotation and aperture, such that zero, one or two simultaneously active pads communicated neutral position, single or combined DoF position, respectively. Like the spatial encoding of Study I (see *Fig. 7a*), the pad activation moved

counterclockwise by starting centrally and moving laterally to indicate higher pronation. A mirrored motion of the same pad indicated increasing supination. The hand aperture was conveyed by activating the pads in the volar sector in the counterclockwise direction. The pad between fifth pronation level and first aperture level was not used in order to ensure that initiation of hand closing was also clearly perceived when the prosthesis was simultaneously fully pronated.

In the novel feedback encoding, see *Fig. 7e*, the forearm was not sectorized to represent the two DoF, but instead the moving sensation induced to represent the spatial modulation of each DoF was coupled so that it was anatomically congruent to the movement of the wrist and fingers (henceforth referred to as the coupled encoding). In this case, two pads were active (except for neutral position) and the same pads conveyed both aperture and rotation levels. As indicated in *Fig. 7e*, the distance between pads conveyed hand aperture while the sequential activation of the pads around the forearm represented wrist rotation. Specifically, active pads rotated counterclockwise and clockwise for pronation and supination with fixed distance between them, respectively, whereas when the hand began closing, the active pads started moving towards the opposite side of the forearm (similar to the hand aperture feedback in Study I, see *Fig. 7a*). To indicate the change in rotation feedback levels more clearly, the stimulation “jumped” two pads to change the level in either direction. The consequence was that, however, some pad activation combinations corresponded to more than one prosthesis state, e.g., hand fully open during fourth pronation or fifth supination level produced the same stimulation pattern. To match the six hand aperture levels in the sectorized encoding, but also to communicate the initial aperture levels more clearly, the first two aperture levels were conveyed by “jumping” across four pads and then by two pads for the subsequent three levels.

In both feedback schemes, the stimulation frequency was set at 35 Hz when no force was applied to ensure clear sensation. First grasp force level (object contact) was indicated by a 200 ms (one window) stimulation burst delivered through the six most dorsally placed pads. To convey the subsequent force levels, the currently active pad(s) (as determined by hand aperture and wrist rotation levels) increased in frequency. However, the maximum frequency needed to be low enough to avoid excessive loss of EMG data due to blanking, which resulted in a narrow range of frequencies available for encoding the force (Study II identified that the entire signal would be blanked at frequencies above 132 Hz when applying common parameter settings). Therefore, amplitude was additionally modulated as it was previously proposed in Study II [2] and [163] to apply simultaneous frequency and amplitude modulation to enhance discriminability of sensations. Second, third and fourth force levels were then conveyed by increasing frequency and amplitude to 50, 65 and 80 Hz and 1.1, 1.2- and 1.3 times the calibrated localization threshold, respectively.

CHAPTER 5. TASKS FOR EVALUATION OF MYOELECTRIC CONTROL PERFORMANCE

In this chapter, it is explained how the subjects were trained in understanding the electro-tactile feedback schemes and how myoelectric control performance was evaluated when controlling a virtual and physical prosthesis, respectively. It is also outlined how the myoelectric control output was mapped into prosthesis motion.

5.1. ONLINE PROSTHETIC CONTROL AND MAPPING

Virtual prosthesis

In Study I and II, the two-DoF control was simulated as a planar cursor control, where the cursor represented prosthesis position (see *Fig. 8a*). The recognized movement class decided the direction of cursor movement, while the contraction intensity set the cursor velocity. The cursor moved down, up, left or right, when the subject performed a closed hand, opened hand, wrist pronation, or wrist supination, respectively. As the tactile feedback was discretized (represented visually as grid cells), visual and tactile feedback were matched by discretizing the visual feedback. This was implemented by hiding the cursor and then highlighting only the grid cell in which the cursor was located (see *Fig. 8b*). The cursor was inactive when the rest class was detected, or when the subject performed a contraction below 20 % of the pMVC of the recognized movement. In Study I, the maximum velocity of the cursor was set so that it took ~2 s to move through the full range of motion of a DoF, as this corresponded to the maximum closing velocity of the Bebionic Hand [25], [131]. For Study II, the maximum velocity of the cursor was decreased so that the full DoF was traversed for ~3 s, which matched the maximum rotation velocity of the Michelangelo Hand [133]. This was done as it was decided that Michelangelo hand would be used in Study III.

Physical prosthesis

In Study III, the control system output was used to command prosthesis movements, i.e., a detection of the supination class caused the supination of the prosthesis wrist etc. As mentioned in *section 2.3*, rotation was represented with twice the number of values compared to aperture but was not equivalently slower to complete full range at maximum velocity. The command input for closing the hand was therefore restricted to 40 % corresponding to ~1.5 s required to close the hand from the fully open position, namely half that of rotation. However, when applying force at 40 % closing velocity, the maximum reachable force value was ~40, decreasing thereby the range of grasping forces that can be produced by 60 %. Therefore, when force was detected

indicating the contact with an object, the maximum command input for the hand was set back to 100 %. Visual feedback that was provided is shown in *Fig. 8c*. The visual feedback was discretized to match the tactile feedback. A rotating bar indicated position levels of the rotation DoF, while a circle that varied in size represented the levels of the aperture DoF. When force was detected the text stating “Aperture” was changed to “Force” and the force level was updated appropriately.

5.2. TRAINING UNDERSTANDING OF FEEDBACK

The subjects were trained in understanding the proprioceptive feedback variables in a similar fashion across all studies. First, the concept of the feedback scheme was introduced verbally by the experimenter. The subject then underwent a structured feedback training divided into two stages: familiarization and reinforced learning. In the familiarization, the subject viewed the cursor in the planar grid (*Fig. 8a*) which was moved discretely by the experimenter from the neutral position to a designated grid cell (feedback level). While viewing the cursor position the subject received electrotactile stimulation, such that the subject could learn to associate the visual feedback with the tactile representation. The cursor moved through transitional grid cells to reach the designated cell and was always reset to neutral position as starting position. Designated positions were all single DoF feedback levels (all grid cells in first row and third column, respectively, see *Fig. 8a*) and all combined DoF feedback levels in fifth row. For combined DoF grid cells, the cursor was moved fully along the wrist rotation DoF before switching to the hand aperture DoF. In the reinforced learning, the subject faced away from the screen. The cursor was moved by the experimenter into a target grid cell, and the subject was then asked to estimate the cursor position based on the received electrotactile stimulation. If the estimation was incorrect, the subject was informed about the correct position, after which the cursor was reset to neutral position and moved into another grid cell. All 24 grid cells were used as targets. The cursor was moved similarly as in the familiarization stage, except that the order of which DoF was moved first varied across trials to avoid biasing the subjects understanding of the feedback. After all targets had been reached, the subject was given a short rest before the reinforced learning was repeated. The order of target cells and DoF movement was updated for the second run.

For Study III, the electrotactile feedback was trained using the visual feedback in *Fig. 8c*. The reinforced learning only included combinations of the two proprioceptive DoFs that did not involve neutral and end positions, e.g., neutral, fully pronated or supinated wrist or fully opened or closed hand (total of 32 target positions). The force feedback was only verbally explained and briefly demonstrated in few positions. The reinforced learning of the force feedback and “trivial” proprioceptive positions were

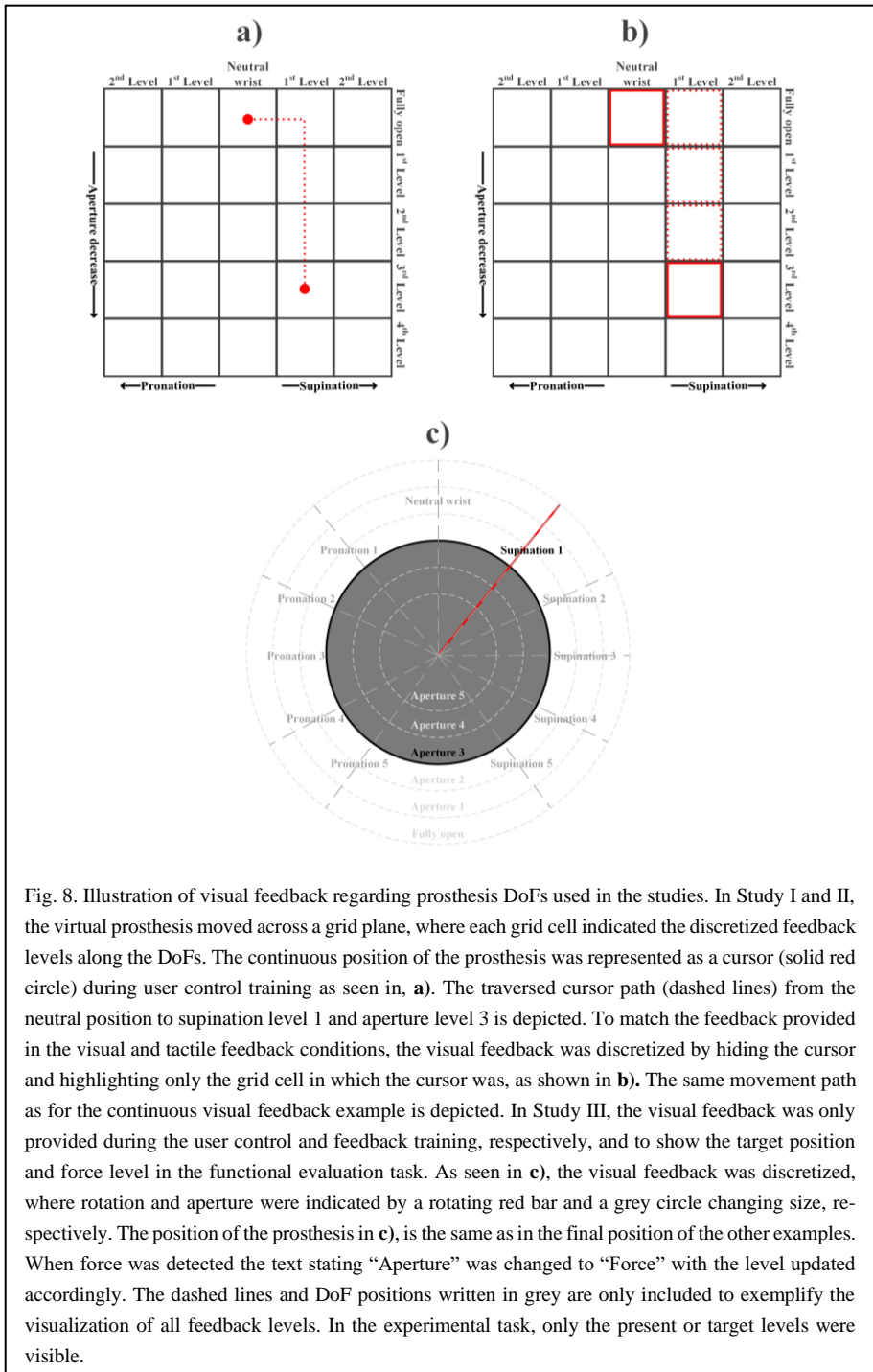


Fig. 8. Illustration of visual feedback regarding prosthesis DoFs used in the studies. In Study I and II, the virtual prosthesis moved across a grid plane, where each grid cell indicated the discretized feedback levels along the DoFs. The continuous position of the prosthesis was represented as a cursor (solid red circle) during user control training as seen in, **a**). The traversed cursor path (dashed lines) from the neutral position to supination level 1 and aperture level 3 is depicted. To match the feedback provided in the visual and tactile feedback conditions, the visual feedback was discretized by hiding the cursor and highlighting only the grid cell in which the cursor was, as shown in **b**). The same movement path as for the continuous visual feedback example is depicted. In Study III, the visual feedback was only provided during the user control and feedback training, respectively, and to show the target position and force level in the functional evaluation task. As seen in **c**), the visual feedback was discretized, where rotation and aperture were indicated by a rotating red bar and a grey circle changing size, respectively. The position of the prosthesis in **c**), is the same as in the final position of the other examples. When force was detected the text stating “Aperture” was changed to “Force” with the level updated accordingly. The dashed lines and DoF positions written in grey are only included to exemplify the visualization of all feedback levels. In the experimental task, only the present or target levels were visible.

excluded to reduce duration of the experiment, as they were deemed simpler to under-

stand compared to the remaining feedback levels and because the experiment duration was already on the verge of being unethical.

5.3. VIRTUAL TARGET REACHING TASK

For Study I and II the control performance was evaluated in a commonly applied target-reaching task [26], [31], [164]–[167]. The task consisted of moving the virtual prosthesis into a target (grid cell highlighted in red) within a 30-s time frame (see *Fig. 8b*). The prosthesis had to dwell inside the target for 1.5 s (2 s for Study II) for the target to be deemed reached and an auditory cue would sound. When the target was reached or the 30 s had expired (no auditory cue), the prosthesis was automatically reset to neutral position and another target appeared. The task ended when all 24 grid cells appeared as targets.

Outcome measures

In the virtual prosthesis control task, the performance was assessed by computing completion rate (percentage of successfully reached targets), time to reach a target (seconds), path efficiency (percentage), distance error (grid cells from target), and number of overshoots. These are common metrics to extract from target-reaching tasks to assess the quality of the control performance [164], [165]. In the optimal scenario, the completion rate is high whereas the duration, path to reach the target, distance error and number of overshoots are low. As the outcome measures were an indication of the performance of reaching a target, they contained information about the two DoFs combined and not individual DoFs independently.

The path efficiency was computed as the shortest possible path to reach the target divided by the actually traversed path. When observing the grid plane in *Fig. 8a*, for single DoF targets, the shortest path was defined as a straight line to the border of the target grid cell. As the control was sequential, for combined DoF targets, the shortest path was defined as straight line to the border of the target in the first DoF and then a straight line to the closest corner of the target grid cell. An overshoot was counted every instance the virtual prosthesis entered the target and exited before the dwell time was realized. The number of overshoots was included as it is an indication of control stability in resting position (drifting motion). When calculating the time to reach a target and path efficiency outcome measures, only successfully reached targets were considered.

To characterize the unsuccessful attempts, the distance error measure was computed. The measure computed the number of grid cells between the position of the virtual prosthesis at the end of the trial and the target grid cell. Thus, the distance error was 1 when the end-position was in a cell adjacent to the target, and 2, if the end-position was in a cell diagonal to the target, as the control was sequential, and the virtual prosthesis therefore needed to traverse two cells to reach the target. The maximal distance

error was then 8, in the case of a target located in a corner grid cell and end-position in the diagonal corner grid cell.

5.4. MULTIFUNCTIONAL PROSTHESIS TASK

In Study III, the myoelectric control performance was evaluated in a functional target-reaching and force-matching task. The evaluation task consisted of 32 trials, where each trial comprised two phases: position and force estimation. Before initiating a trial, the prosthesis was reset to neutral position. During the position phase, the subject faced the contralateral side towards the monitor to avoid looking at the prosthesis (see *Fig. 9a*) while a position target was displayed on the screen (see *Fig. 8c*). The subject then had to rely on the tactile feedback to reach the target position (no visual feedback available in the position phase). The position targets were the 32 “non-trivial” positions from the reinforced learning. When the subject determined that the correct position was reached, he/she indicated this verbally and the force phase was initiated by showing a force target (either second or third force level) on the monitor. The subject had to reach the indicated force level by grasping one of three rigid wooden balls (see *Fig. 9b*). Rigid objects were used to avoid force estimation from visual feedback (deformation of compliant object). The largest ball could be grasped at fully opened hand and first aperture level, the medium at second and third level, and the smallest at fourth level and the widest opening of the fifth level. If the hand was fully closed following the position phase, the subject opened the hand to fit the smallest ball. The spherical shape of the object was selected as it could be grasped at any orientation. As for the position phase, when the subject determined that the correct level was reached, it was implied verbally, and the trial finished. In order to maintain the flow of the evaluation task, the subject performance was not penalized if the prosthesis moved during grasping or that the wrong ball size was grasp. Neither phase had any time constraint.

Outcome measures

In the multifunctional prosthetic control task, the performance was assessed through the distance error and time spent per trial phase. As the subjects were not automatically informed whether a target was reached (e.g., auditory cues in the virtual target-reach task), the computation of the outcome measures considered both unsuccessful and successful attempts. The error was calculated directly for each feedback variable (e.g., one outcome for hand aperture, wrist rotation and grasp force, respectively) as levels off the target, and the spend time was calculated per trial phase (e.g., one outcome for the position and force phase, respectively).

5.5. STATISTICAL ANALYSIS

The respective outcome measures for each study were calculated for each trial and averaged across all trials for each individual subject and each feedback condition. Kolmogorov-Smirnov test for normality showed that no data groups (experimental

conditions) belonged to the normal distribution, and therefore only non-parametric statistical analyses were applied. Friedman test was used to assess if there was a statistically significant difference in the group of conditions and Tukey-Kramer's honestly significant difference procedure was applied for post-hoc pair-wise comparisons if a significant effect was detected. Wilcoxon signed rank test was applied in case there was only two conditions to compare. The significance level was set to $p < 0.05$. The descriptive results are reported as median/interquartile range.

CHAPTER 6. MAIN RESULTS

This chapter recalls the aim and provides the experimental protocol (description of test conditions) and main outcomes of each of the three studies. In all studies, before initializing the experiment, the subjects carefully read and signed a consent form. The experimental protocols were approved by the local ethical committee of Region Nordjylland (approval number: N-20 150 075).

6.1. TWO-DOF POSITION INFORMATION CAN BE PROVIDED EFFECTIVELY THROUGH EITHER SPATIAL OR AMPLITUDE MODULATED ELECTROTACTILE FEEDBACK

Aim

The electrotactile technology is versatile in how to modulate stimulation for communication of feedback variables as either intensity, frequency, timing, or location of the stimulation can be adjusted. In the literature, different modulation strategies have been applied but they have rarely been directly compared to assess whether there is a preferred mode to convey the DoFs of a multifunctional prosthesis. For Study I, two novel feedback coding schemes based on amplitude and spatial modulation, respectively, were designed to communicate the proprioceptive information of wrist rotation and hand aperture of a virtual prosthesis and compare how they affect myoelectric control performance.

Experimental protocol

Thirteen subjects (age in mean \pm standard deviation: 34.4 ± 11.6 years; gender: 1 female, 12 male; handedness: 1 left-handed, 12 right-handed) were recruited. The experiment was a single session of 2-3 hours duration. Three test conditions were evaluated: visual, spatial, and amplitude-based feedback (see *section 4.2* and *Fig. 7a* and *b* for visual depiction of the feedback encodings). The visual feedback was the benchmark condition as the vision provides, as outlined in *section 1.3*, the most accurate state estimation.

Initially, the equipment was placed as visualized in *Fig. 2a*, respectively, and the electrodes were carefully positioned as described in *section 3.2* and *4.1*. The skin was cleansed with alcohol swaps and moistened with water to improve sticking of the hydrogel to the skin. No further skin preparation was conducted to better imitate quick everyday preparation of prosthesis use. For the remaining experiment duration, the subject was seated comfortably in a chair with the arms relaxed down the side of the torso as depicted *Fig. 10a*.

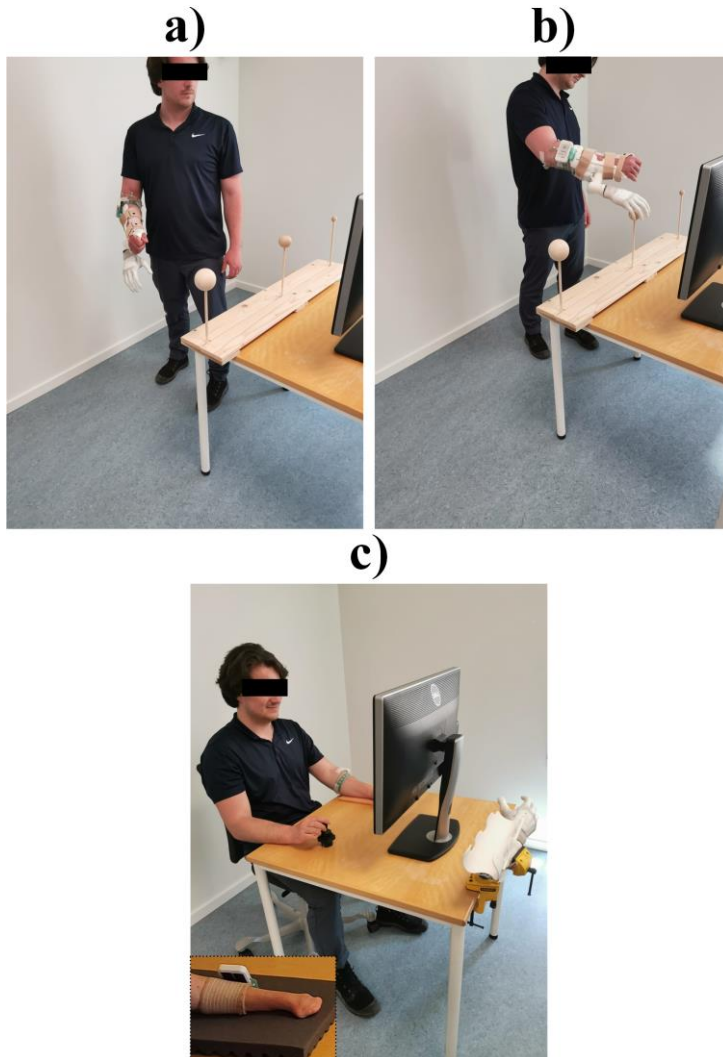


Fig. 9. The illustrations of the setup used in the experimental protocol of Study III. In **a)**, the subject performed the position phase of a trial during the evaluation task, where the target position was indicated on the monitor while visual feedback of the prosthesis was occluded. In **b)**, the subject reached the force phase, where the appropriate ball size was grasped, and target force estimated. The capture in **c)** shows the experimental setup used by the amputee subject. The setup is hereby demonstrated by an able-bodied subject, while the inset in bottom left corner shows the position of the electrode in the amputee participant. The stimulation equipment was worn on the residual limb in a similar manner as in Study I (see *Fig. 8a*). The prosthesis was occluded from vision and controlled with the contralateral hand using a joystick.

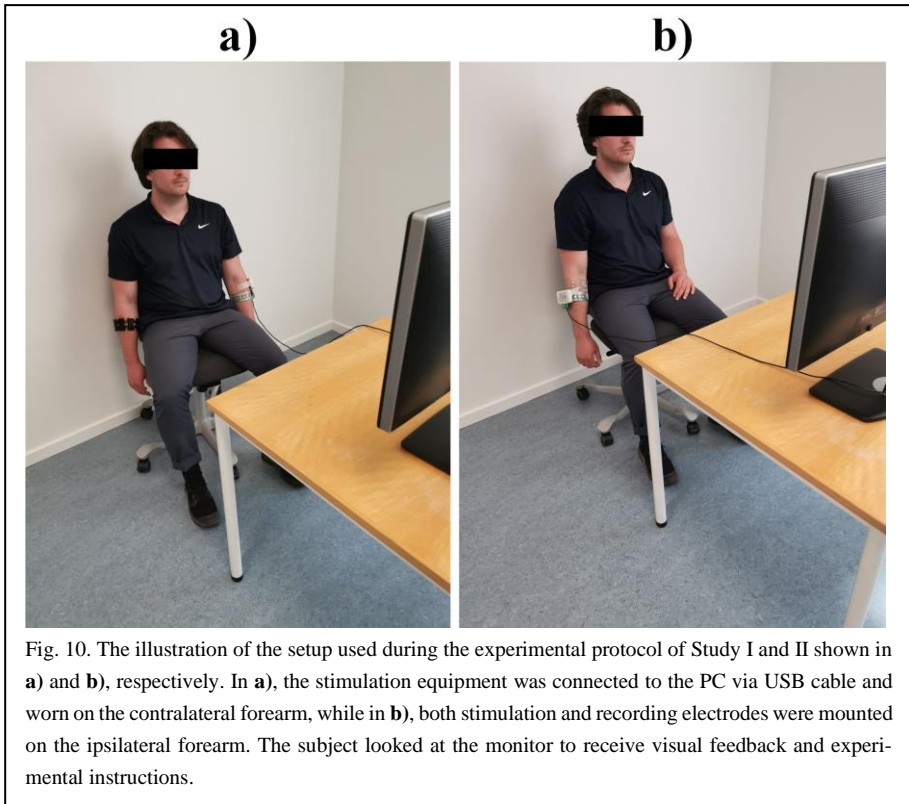


Fig. 10. The illustration of the setup used during the experimental protocol of Study I and II shown in **a)** and **b)**, respectively. In **a)**, the stimulation equipment was connected to the PC via USB cable and worn on the contralateral forearm, while in **b)**, both stimulation and recording electrodes were mounted on the ipsilateral forearm. The subject looked at the monitor to receive visual feedback and experimental instructions.

The myoelectric control was calibrated as described in *Chapter 3* and the movement direction and velocity of the virtual prosthesis was mapped as described in *section 5.1*. The subject then briefly trained the sequential myoelectric control of the virtual prosthesis. First by receiving continuous visual feedback of the prosthesis (cursor seen in *Fig. 8a*) and then discrete visual feedback (highlighted grid cell seen in *Fig. 8b*) which matched the discretization of the tactile feedback. The subject trained until the experimenter determined that the control was stable (no more than five minutes for each visual feedback representation). Following the myoelectric control training, the subject completed the target-reaching task (as described in *section 5.3*) for the visual feedback condition relying only on the discrete visual feedback.

The subject was then trained in understanding one of the two feedback encodings (amplitude or spatial modulation) as described in *section 5.2*. Afterwards, the myoelectric control and feedback were combined, and the subject briefly trained the understanding of the feedback combined with control by freely moving around the virtual prosthesis. The control performance was then evaluated in the target-reaching task, where the visual feedback was removed and only the discrete tactile feedback was received. After completing evaluation of one feedback encoding, the procedure was repeated for the other. The order of which feedback scheme was evaluated first, was

counterbalanced between subjects. The computation of distance error was omitted for the visual condition, as the control only comprised three unsuccessful attempts across all subjects. The number of overshoots was not computed for Study I.

Main outcomes

The summary results from Study I are shown in *Fig. 11*. No difference in control performance was detected between the two tactile conditions for any outcome measure. The subjects were able to effectively understand two independent feedback variables communicated simultaneously while also controlling the prosthesis. This is a promising outcome demonstrating that there is a flexibility in designing useful feedback encodings. A user could quickly test both feedback coding schemes and decide which one is preferred or even mix the representation of DoFs (e.g., aperture from the spatial scheme and rotation from the amplitude scheme).

As anticipated, the visual condition (superior sense in sensorimotor control) outperformed both tactile conditions in terms of completion rate ($p < 0.001$, visual: 100/0% vs spatial: 94/10%; and $p < 0.01$, visual vs amplitude: 94/2%) and time to reach a target ($p < 0.01$, visual: 7/2 s vs spatial: 9/2 s; and $p < 0.001$, visual vs amplitude: 10/3 s). However, the path efficiency was similar across all conditions (visual: 46/13%, spatial: 51/10%, and amplitude: 47/14%) indicating that when the tactile feedback was understood (successful trials), it was as useful as visual feedback for accurate estimation of control actions needed to reach the target. Additionally encouraging was that

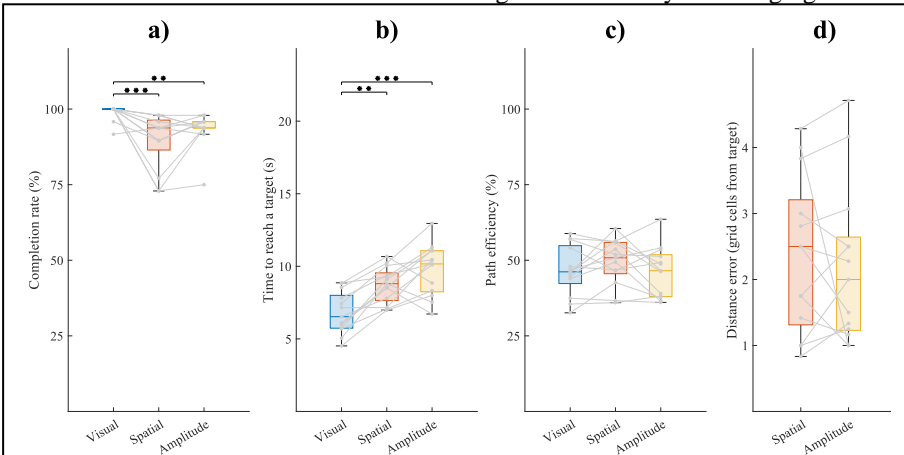


Fig. 11. Box plot visualization of the summary results from Study I. The outcome measures of completion rate, time to reach a target, path efficiency, and distance error are shown in **a)**, **b)**, **c)**, and **d)**, respectively. The blue, red, and yellow box plots show the results from the visual, spatial, and amplitude conditions, respectively. The distance error for the visual feedback condition was omitted as the completion rate was near flawless. The horizontal line, box limits, whiskers, grey dots, and connecting grey lines indicate median, interquartile range, extreme values, subject-specific outcomes connected between conditions, respectively. The asterisks indicate p-values, where *, **, and *** correspond to $p < 0.05$, $p < 0.01$, and $p < 0.001$, respectively. The significance level was $p < 0.05$.

when the target was not reached, the median distance error was only ~ 2 for both tactile conditions (spatial: 2.5/1.9 and amplitude: 2/1.4 grid cells from the target), and therefore the end-position was actually close to the target level. The time efficiency was worse for the tactile conditions, likely due to the need for longer cognitive processing to interpret a new and less trained source of sensory information. The high performance achieved in the tactile condition is even further impressive when considering the short training duration (<30 min) spend to understand the feedback encoding, and with a longer training the completion rates could even approximate that of visual feedback.

6.2. FIRMWARE BLANKING OF STIMULATION ARTEFACTS FACILITATES STABLE CLOSED-LOOP MYOELECTRIC CONTROL WHEN PLACING ELECTRODES IPSILATERALLY

Aim

Compared to vibrotactile stimulation, electrotactile stimulation is less applied in the literature to convey the state of a myoelectric prosthesis. The electrical pulses contaminate the EMG recording and disrupt the prosthetic control, which makes electrotactile stimulation a less practically applicable solution for communicating feedback variables. Blanking of the electrical artefact have shown to be an effective strategy to increase classification accuracy in offline analysis. In Study II, the aim was to demonstrate that online blanking of stimulation artefacts can facilitate stable myoelectric control while electrotactile stimulation is delivered adjacently to the recording electrode. A novel feedback encoding scheme was designed to convey useful feedback while simultaneously maximally stressing the control signal by modulating the length and frequency of blanked intervals as well as the recording channels that are affected by online artefacts.

Experimental protocol

In Study II, 10 subjects (age: 27.1 ± 2.4 years; gender: 2 female, 8 male; handedness: all right-handed) were recruited. The experiment contained three test conditions, namely, visual feedback, combined visual and tactile feedback, and tactile feedback (see *section 4.3* and *Fig. 7c* for visual depiction of the feedback encoding). The combined visual and tactile condition was included to directly evaluate whether the stimulation influenced the control stability compared to the visual condition only. The aim of the condition with tactile feedback only was to demonstrate that the designed encoding scheme provided useful information to the participant that could be exploited for control. The equipment was carefully positioned on the ipsilateral forearm (see *Fig. 2b*) and the subject sat relaxed in a chair for the remaining time as shown in *Fig. 10b*. Otherwise, Study II followed the same experimental protocol as Study I (see *section 6.1*), except that the performance of all conditions was evaluated consecutively (in the same order as listed above) with 3-5 minutes break in between conditions. For

the combined visual and tactile condition, it was assumed that the subject would ignore the tactile feedback and only utilize the visual feedback to estimate prosthesis position. As explained before, the tactile feedback was added in this case only to stress the control. Therefore, the conditions were not counterbalanced across subjects. The distance error was not computed, but the number of overshoots was included as it is an indication of control stability, which was useful to consider when evaluating potential interference introduced by the electrical stimulation.

Main outcomes

Summary results from Study II is shown in *Fig. 12*. The visual and combined visual and tactile conditions did not differ in performance for any outcome measure and were characterized by overall high performance, highlighted by the near flawless completion rate (visual: 100/4%, combined: 100/4%,). This result indicates that the firmware blanking of stimulation artefact and following signal processing facilitated stable online closed-loop myoelectric control when stimulation and recording electrodes were placed adjacently on the same arm. This a highly encouraging results for the prospect of delivering multivariable somatosensory information to myoelectric prosthesis users through a compact electro tactile stimulation display.

Similarly, as in Study I, the completion rate (78/25%) and time to reach a target (13/4 s) was significantly worse in the tactile condition compared to the visual conditions. The path efficiency (38/8%) and number of overshoots (0.5/0.4) were similar to the visual conditions indicating a high performance considering the disadvantage of only receiving tactile feedback. However, the absolute values of the outcome measures (completion rate, time to reach a target and path efficiency) are notably worse for the

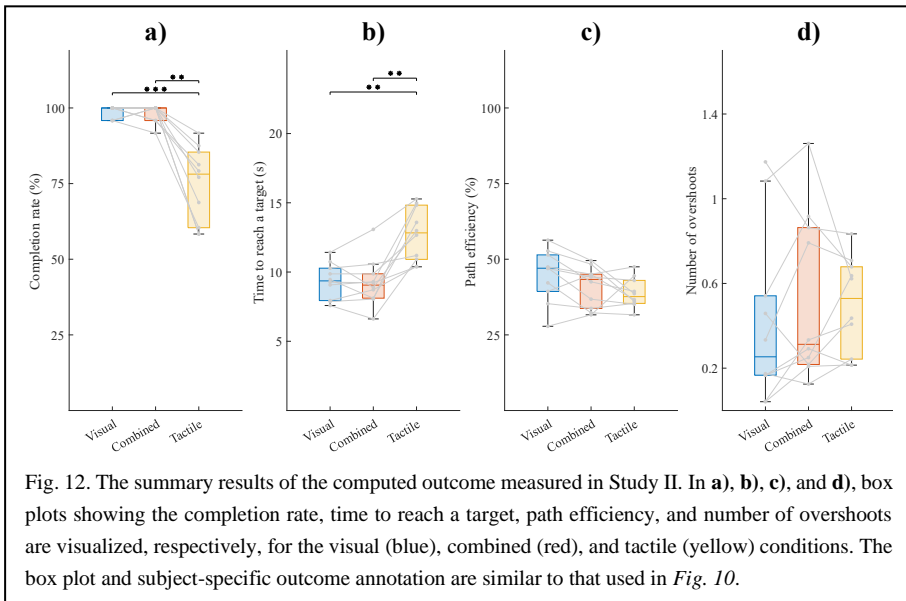


Fig. 12. The summary results of the computed outcome measured in Study II. In **a**), **b**), **c**), and **d**), box plots showing the completion rate, time to reach a target, path efficiency, and number of overshoots are visualized, respectively, for the visual (blue), combined (red), and tactile (yellow) conditions. The box plot and subject-specific outcome annotation are similar to that used in *Fig. 10*.

tactile condition in Study II than the values achieved in both tactile conditions in Study I. This could be an indication that the mixed feedback encoding was more difficult to understand. However, the training in understanding the feedback was identical for Study I and II and the reinforced learning showed a similar success rate between the three encodings (spatial: 75/22%, amplitude: 79/14, and mixed: 74/13%). Another speculation could therefore be that control instability caused by the electrical stimulation interference was more pronounced when no visual feedback was available.

6.3. PROVISION OF SUPPLEMENTARY FEEDBACK DURING MYOELECTRIC CONTROL IMPROVES POSITION ESTIMATION OF A MULTIFUNCTIONAL PROSTHESIS

Aim

The incidental feedback produced by the moving parts of a myoelectric prosthesis contain information about the prosthesis's state. In the previous two studies delivering non-invasive stimulation to convey two feedback variables simultaneously, the subjects did not wear the prosthesis and therefore, it could not be tested if the supplementary feedback is more informative than the baseline of incidental feedback (without vision). Furthermore, no previous study has simultaneously communicated the full state of the prosthesis in a single coding scheme. Therefore, in Study III, a novel feedback scheme was designed that spatially imitated the movement of the wrist and fingers during rotating and hand closing/opening providing thereby anatomically congruent feedback. The full closed-loop setup including the physical prosthesis was placed on the ipsi-lateral forearm and the myoelectric control performance was evaluated in a functional task.

Experimental protocol

In Study III, 10 able-bodied (age: 34.4 ± 11.6 years; gender: 2 female, 8 male; handedness: all righthanded) and a congenital left-hand limb-deficient subject (56 years, female) were recruited. The experiment included three test conditions: incidental, sectorized and coupled feedback (see *section 4.4* and *Fig. 7d* and *e* for visual depiction of the feedback encodings) and consisted of a two-session experiment of approximately two to three hours duration in each session. The sessions were conducted on two consecutive days. The first session was dedicated to stimulation calibration and training the understanding of the two feedback encodings, as explained in *section 5.4*, and the subjects therefore only wore the stimulation electrode. At the end of the first session, the placement of the stimulation electrode was marked to use the same placement in the second session with the intention of reducing calibration duration. The order of training of feedback schemes was counterbalanced between subjects.

In the second session, the myoelectric control performance was evaluated in a functional target-reaching and force-matching task. First, the full closed-loop control setup

was mounted as shown in *Fig. 2c* and the stimulation intensity was adjusted using the amplitude values determined in the first session as an informed starting point. Then, the myoelectric control was calibrated and briefly trained. The performance of each of the three conditions was evaluated with the order counterbalanced between subjects. For the electrotactile feedback conditions, the feedback encoding was first trained in combination with the myoelectric prosthetic control. The subject could practice freely until it was deemed by the experimenter that the control was stable, and the understanding of the feedback was sufficient. This step lasted for maximally 10 minutes. It was important that the closed-loop control was robust, so that poor control was not responsible for the eventual difference in performance across feedback conditions. The subject could control both DoFs simultaneously but was neither encouraged nor discouraged to do so. The evaluation task consisted of 32 trials with a two-minute break after a set of eight trials to reduce fatigue.

The amputee subject completed a similar protocol. However, it was not possible to fit even the smallest recording electrode size on the residual limb, but only the smallest stimulation electrode. As a compromise, the prosthesis was placed on table in a vice outside the view of the subject and was controlled using a joystick (see *Fig. 9c*) where left/right and up/down corresponded to wrist pronation/supination and hand opening/closing, respectively. The velocity/force of the prosthesis was proportional to how far in each direction the lever was pushed. The protocol was compressed into a single session of 2.5 hours comprising familiarization, a single run of reinforced learning, training of closed-loop control and evaluation of coupled feedback before repeating the same procedures for the sectorized feedback. The condition with incidental feedback was omitted as the subject did not wear the prosthesis. The outcome measures computed for the amputee subject were not included in the statistical analysis but were considered separately.

Main outcomes

The summary results from Study III are shown in *Fig. 13*. Most importantly, there was no difference between electrotactile feedback conditions in terms of myoelectric prosthetic control performance. The reinforced learning did indicate a significantly greater understanding of the sectorized encoding in both the rotation DoF ($p < 0.01$, sectorized: 0.2/0.1 levels vs coupled: 0.5/0.3 levels) and aperture DoF ($p < 0.001$, sectorized: 0.1/0.1 levels vs coupled: 0.3/0.2 levels), but this effect was eliminated when adding the myoelectric control. It is likely that the anatomically congruent motion of the stimulation was easier to interpret when the prosthesis was included to visually match the perceived tactile feedback.

The target distance error was significantly lower for the electrotactile feedback conditions compared to the incidental feedback condition for both the rotation DoF ($p < 0.05$, incidental: 0.8/0.6 levels vs sectorized: 0.4/0.3 levels; and $p < 0.01$, incidental

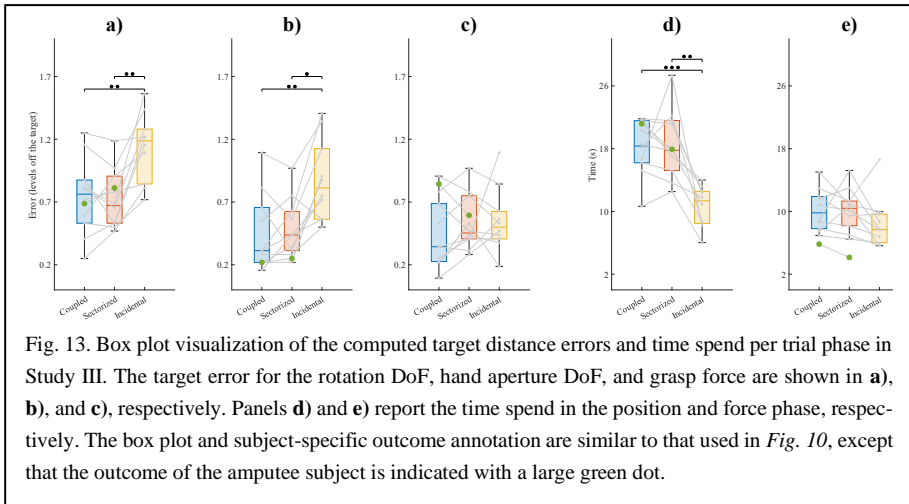


Fig. 13. Box plot visualization of the computed target distance errors and time spend per trial phase in Study III. The target error for the rotation DoF, hand aperture DoF, and grasp force are shown in **a)**, **b)**, and **c)**, respectively. Panels **d)** and **e)** report the time spend in the position and force phase, respectively. The box plot and subject-specific outcome annotation are similar to that used in Fig. 10, except that the outcome of the amputee subject is indicated with a large green dot.

vs coupled: 0.3/0.4 levels) and the aperture DoF ($p < 0.01$, incidental: 1.2/0.4 levels vs sectorized: 0.7/0.4 levels; and incidental vs coupled: 0.8/0.3 levels). The provision of the explicit electro-tactile feedback can therefore be used to estimate the position of the prosthesis more efficiently. However, the increased accuracy compromises the time, as the duration spend to estimate the position was significantly longer for the electro-tactile feedback conditions compared to the incidental feedback condition ($p < 0.01$, incidental: 11/4 s vs sectorized: 18/6 levels; and $p < 0.001$, incidental vs coupled: 18/5 s). It could seem that the subjects used more time to “listen” to the explicit electro-tactile information and applied it actively to adjust control actions compared to the rough incidental feedback that contains less precise information about the prosthesis state. While the electro-tactile feedback did improve the position accuracy, the performance in the incidental feedback condition was still decent with median error of ~ 1 level in both DoFs, emphasizing that the incidental feedback is a useful source of information for estimating the prosthesis’ state. The target distance error and time spend in the force phase were similar between the two conditions, and therefore, somewhat surprisingly the supplemental feedback did not improve force control compared to incidental feedback only. The force feedback variable was also divided into fewer levels than the aperture and rotation DoF, and an increase in number of levels could maybe have facilitated significant higher accuracy compared to the incidental condition. The results of the amputee subject (green dots) followed the same trend as the able-bodied subjects.

CHAPTER 7. CONCLUSIONS

In *section 1.5.1*, the research questions were formulated to investigate open challenges and fill the gaps in the state of the art. The three studies comprising the PhD project were designed and conducted, as an effort towards addressing the posed questions. Below, we explain how the findings from the three studies provide qualified answers to the research questions, effectively synthesizing the work of the project.

RQ1. How can multiple feedback variables be communicated in a single feedback coding scheme using a single stimulation display to improve myoelectric control performance? Do the subjects find specific modulation of the stimulation more intuitive to understand than others?

To answer the first question, five different feedback coding schemes were designed and evaluated in myoelectric control tasks. In the three project studies, it was shown that the subjects could successfully interpret the provided feedback and actively apply it during online myoelectric control. In Study I, two novel schemes were developed to communicate the two DoFs of wrist rotation and hand aperture through either amplitude or spatial modulation. In Study II, the same DoFs were communicated by a novel mixed modulation scheme, where wrist rotation and hand aperture were represented spatially and by parameter modulation, respectively. In Study III, novel feedback encodings were developed to communicate the full state of a multifunctional myoelectric prosthesis where proprioceptive information was modulated spatially while grasp force was conveyed by parameter modulation. In one scheme, the spatial movement of the stimulation was anatomically congruent to the motion of the prosthesis' wrist and fingers, and in the other the information describing each DoF was delivered via dedicated sections of the forearm. Thus, five different ways to modulate the feedback variables comprising the prosthesis' state were demonstrated and showed to provide useful information during evaluation of myoelectric control performance. **The studies provide practical demonstration of the flexibility of multi-channel electrotactile stimulation interface where multiple feedback variables can be mapped in different ways to create easily interpretable stimulation profiles, using a limited area of the skin (cross-section of the forearm).**

To answer the second question in **RQ1**, the feedback schemes designed for Study I and III, were compared, respectively. When interpreting the feedback psychometrically, there was no difference between amplitude and spatially modulated feedback in Study I, and the similar performance was observed when the two encoding methods were evaluated in a closed-loop myoelectric control task. In Study III, the sectorized feedback scheme was easier to understand in the psychometric evaluation compared to the anatomically congruent feedback. However, the difference was evened out when the schemes were combined with online myoelectric control of a multifunctional prosthesis. Thus, in the practically meaningful evaluation, the two feedback coding

schemes were showed to be similarly effective in conveying the feedback variables. **Thus, the electrotactile communication of multiple feedback variables is not only flexible, but the encoding methods are similarly effective in terms of decoding and online control performance. Therefore, we have flexibility in choosing the encoding: one could show different schemes to potential users, and they could then select what they find most intuitive.**

RQ2. Compared to myoelectric control without electrical interference, can online blanking of stimulation artefacts facilitate similarly stable control while receiving electrotactile feedback with stimulation and recording electrodes placed adjacently?

Study II was conducted to answer the question posed in **RQ2**. A device that comprised both an electrotactile stimulation and EMG recording unit with integrated firmware blanking of stimulation artefacts was used for the purpose of evaluating myoelectric control of a virtual prosthesis with and without receiving concurrent electrotactile stimulation. The novel mixed encoding scheme successfully communicated the two DoFs wrist rotation and hand aperture in a myoelectric control task, while maximally stressing the control by modulating recording channels affected by the stimulation as well as the length and frequency of the blanking intervals. The online blanking of electrical stimulation pulses facilitated stable myoelectric control when stimulation and recording electrodes were placed adjacently on the same forearm. Thus, the answer to the question is yes, the online blanking of stimulation artefacts can be effectively applied to enable the use of electrotactile stimulation in closed-loop myoelectric control. **This allows using the flexibility of the electrotactile interface, as explained in RQ1, to develop closed-loop systems integrated in the prosthesis socket.**

RQ3. Can the full state of a multifunctional myoelectric prosthesis be effectively communicated to the user during a functional task? How is the control performance when receiving electrotactile feedback compared to incidental feedback from the prosthesis?

To answer the first question, the two feedback coding schemes conveying wrist rotation, hand aperture and grasp force were developed in Study III. The subjects wore the entire closed-loop control setup on the ipsilateral forearm while performing a functional target-reaching and force-matching task. The novel anatomically congruent feedback was compared to the previously evaluated sectorized feedback (Study I) and showed similarly high effectiveness in terms of myoelectric control performance. This therefore demonstrates that the full state of the multifunctional prosthesis can be successfully communicated through various feedback encodings. **The versatility of the feedback encodings in all the studies underlines the flexibility of the electrotactile technology. The detailed feedback information can be communicated by a slim electrode array through a device that facilitates stable closed-loop myoelectric**

control during simultaneous stimulation and recording. This is an important step towards accommodating the functionality of an advanced prosthesis with the somatosensory feedback that can match the dexterity of the control.

To answer the second question in **RQ3**, an incidental feedback condition (without vision) was included in the experimental protocol of Study III. Compared to receiving only incidental feedback, the accuracy of estimating the position (rotation and aperture) of the prosthesis was higher during provision of explicit electro tactile information. However, the time spend to estimate the position was equivalently slower when receiving the electro tactile stimulation, indicating a need for longer duration to process information contained in the supplementary feedback. In the force-matching task, the performance was similar between incidental and electro tactile conditions. **Thus, the explicit electro tactile feedback improves estimation of prosthesis position compared to incidental feedback, but as the electro tactile stimulation is more detailed, more information needs to be interpreted which compromises the task duration. With more elaborate and longer training, the feedback might be better integrated in the user’s internal model, and the time needed for interpreting the feedback would likely decrease. It was demonstrated that that the subjects could adjust the prosthesis position without looking at it. In common daily life activities, the amputees need to look at the hand all the time, and it is therefore anticipated that the proposed feedback could decrease this reliance of vision, after provision of appropriate training in e.g., home-use study.**

The PhD project presented a functional evaluation of myoelectric control performance using an equipment placement that approximated how actual upper-limb myoelectric prosthetic users would wear the prosthesis. Thereby, a solution is provided to the long-standing problem of electro tactile stimulation, which is not applicable in closed-loop myoelectric control with the full setup placed together on the same forearm. The natural next step will then be to move the assessment outside the controlled laboratory environment to evaluate the impact of the multivariable feedback in e.g., home-use and assess long-term effects. The closed-loop control system then needs to be embedded in the prosthesis socket in a self-contained solution as visualized in *Fig. 14*. The closed-loop control system validated in the PhD project is compact, and the multi-channel electrode array used to provide multiple somatosensory feedback variables simultaneously and effectively is slim, and therefore comprise hardware that can be easily integrated in the prosthesis socket as exemplified in *Fig. 14*. However, before initiating more extensive evaluations it would be beneficial to further investigate certain aspects of the presented application.

7.1. FUTURE CHALLENGES

In the studies comprising the PhD project, all hardware units were interfaced through a laptop computer in which the control system was implemented. However, the Max

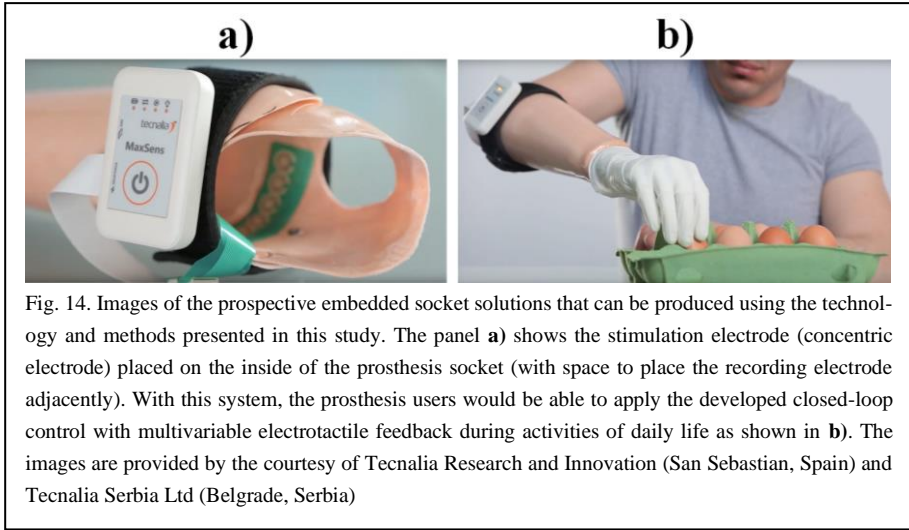


Fig. 14. Images of the prospective embedded socket solutions that can be produced using the technology and methods presented in this study. The panel **a)** shows the stimulation electrode (concentric electrode) placed on the inside of the prosthesis socket (with space to place the recording electrode adjacently). With this system, the prosthesis users would be able to apply the developed closed-loop control with multivariable electrotactile feedback during activities of daily life as shown in **b)**. The images are provided by the courtesy of Tecnalía Research and Innovation (San Sebastian, Spain) and Tecnalía Serbia Ltd (Belgrade, Serbia)

Sens device contains enough processing power to also have the control system implemented on the embedded platform. Since both the Michelangelo Hand and MaxSens device contain Bluetooth modules allowing direct wireless communication, the laptop interfacing could be removed, and the prosthesis system would then be truly self-contained. Such implementation would likely also increase stability of inter-unit communication and decrease processing duration as there would be less data streaming. Of course, the ultimate solution would be to have both myoelectric control system and the control of prosthesis motors integrated into a single interface.

Currently, calibrating the electrotactile stimulation intensity is time demanding. Determining amplitude values for individual pads that produce pleasant and similar sensation intensity across pads is a tedious process that requires careful attention for the stimulation to reach the full potential. For a technology to be compelling to use, it must not require too long time to set up. A strategy to address this issue could be to calibrate stimulation intensity based on a measurable parameter, e.g., skin impedance, rather than the subjective iterative process that the current calibration procedure require. A previous study showed that skin impedance can be a descriptive measure for controlling sensation intensity during activities of daily life when the electrode patch partially detaches from the skin [112]. It could be investigated whether skin impedance is also a good general measure for calibrating sensation intensity. Another approach would be to develop procedures for fast calibration where the psychometric parameters measured from a few pads could be used to estimate the values for the rest of the electrode pads [113].

While the blanking artefacts suppressed the interference of electrical stimulation pulses, it is clear that current leakage is still present in the EMG recording. The stimulation electrode consisted of smaller circular pads and a large, elongated reference pad. A concentric electrode design, where the reference electrode surrounds the active

pads is known to ensure a more superficial current flow that decrease current spread [110]. Actually, a concentric version of the 16-channel electrode array used in the present PhD project was produced previously [116] (see also *Fig. 14a*). It would be beneficial to compare the presence of stimulation artefacts in the EMG recording when using the two electrode designs and investigate whether the concentric design could further improve the stability of the closed-loop myoelectric control.

It was shown that when using the stimulation parameter settings for the feedback encoding in Study II, the recording would be entirely blanked when stimulating with frequencies above 132 Hz, establishing an upper frequency limit. While the feedback encoding was designed to stress the control system, it was not directly evaluated how large is a percentage of EMG recording that could be blanked while still retaining reliable online control [127]. It would be useful to identify such limitations for the prospect of designing feedback encodings that could be applied practically in closed-loop myoelectric control.

As a last remark, in the present project all feedback encoding methods conveyed discrete levels of the feedback variables. The advantage of this approach is that the encodings are simpler to learn and interpret by the participants, but the feedback is limited in resolution. It would be therefore relevant to investigate whether there is an optimal discretization of each feedback variable to improve the control performance in activities of daily life compared to incidental feedback, and whether the optimal discretization changes depending on how the stimulation is modulated.

CHAPTER 8. LITERATURE LIST

- [1] M. A. Garenfeld, C. K. Mortensen, M. Strbac, J. L. Dideriksen, and S. Dosen, “Amplitude versus spatially modulated electrotactile feedback for myoelectric control of two degrees of freedom,” *J. Neural Eng.*, vol. 17, no. 4, pp. 1–15, 2020.
- [2] M. A. Garenfeld *et al.*, “A compact system for simultaneous stimulation and recording for closed-loop myoelectric control,” *J. Neuroeng. Rehabil.*, vol. 18, no. 1, pp. 1–17, 2021.
- [3] M. A. Garenfeld, M. Strbac, N. Jorgovanovic, J. L. Dideriksen, and S. Dosen, “Closed-Loop Control of a Multifunctional Myoelectric Prosthesis With Full-State Anatomically Congruent Electrotactile Feedback,” *IEEE Trans. Neural Syst. Rehabil. Eng.*, vol. 31, pp. 2090–2100, 2023.
- [4] J. W. Sensinger and S. Dosen, “A Review of Sensory Feedback in Upper-Limb Prostheses From the Perspective of Human Motor Control,” *Front. Hum. Neurosci.*, vol. 14, no. June, pp. 1–24, 2020.
- [5] P. Svensson, U. Wijk, A. Björkman, and C. Antfolk, “A review of invasive and non-invasive sensory feedback in upper limb prostheses,” *Expert Rev. Med. Devices*, vol. 14, no. 6, pp. 439–447, Jun. 2017.
- [6] C. Antfolk *et al.*, “Sensory feedback in upper limb prosthetics,” *Expert Rev. Ltd*, vol. 10, no. 1, pp. 45–54, Jan. 2013.
- [7] J. S. Schofield, K. R. Evans, J. P. Carey, and J. S. Hebert, “Applications of sensory feedback in motorized upper extremity prosthesis: A review,” *Expert Rev. Med. Devices*, vol. 11, no. 5, pp. 499–511, Sep. 2014.
- [8] B. Stephens-Fripp, G. Alici, and R. Mutlu, “A review of non-invasive sensory feedback methods for transradial prosthetic hands,” *IEEE Access*, vol. 6, pp. 6878–6899, 2018.
- [9] R. S. Johansson and J. R. Flanagan, “Coding and use of tactile signals from the fingertips in object manipulation tasks,” *Nat. Rev. Neurosci.*, vol. 10, no. 5, pp. 345–359, 2009.
- [10] B. Gesslbauer, L. A. Hruby, A. D. Roche, D. Farina, R. Blumer, and O. C. Aszmann, “Axonal components of nerves innervating the human arm,” *Ann. Neurol.*, vol. 82, no. 3, pp. 396–408, 2017.

- [11] K. Østlie, P. Magnus, O. H. Skjeldal, B. Garfelt, and K. Tambs, “Mental health and satisfaction with life among upper limb amputees: A Norwegian population-based survey comparing adult acquired major upper limb amputees with a control group,” *Disabil. Rehabil.*, vol. 33, no. 17–18, pp. 1594–1607, 2011.
- [12] A. Saradjian, A. R. Thompson, and D. Datta, “The experience of men using an upper limb prosthesis following amputation: Positive coping and minimizing feeling different,” *Disabil. Rehabil.*, vol. 30, no. 11, pp. 871–883, 2008.
- [13] C. L. McDonald, S. Westcott-McCoy, M. R. Weaver, J. Haagsma, and D. Kartin, “Global prevalence of traumatic non-fatal limb amputation,” *Prosthet. Orthot. Int.*, vol. 45, no. 2, pp. 105–114, 2021.
- [14] K. Ziegler-graham, E. J. Mackenzie, P. L. Ephraim, T. G. Travison, and R. Brookmeyer, “Estimating the Prevalence of Limb Loss in the United States : 2005 to 2050,” *Arch Phys Med Rehabil*, vol. 89, no. 3, pp. 422–429, 2008.
- [15] M. P. Fahrenkopf, N. S. Adams, J. P. Kelpin, and V. H. Do, “Hand Amputations,” *Eplasty*, vol. Sep 28, no. 18:ic21, pp. 1–6, 2018.
- [16] B. Maat, G. Smit, D. Plettenburg, and P. Breedveld, “Passive prosthetic hands and tools : A literature review,” *Prosthet. Orthot. Int.*, vol. 42, no. 1, pp. 66–74, 2018.
- [17] D. H. Plettenburg, “The WILMER passive hand prosthesis for toddlers,” *J. Prosthetics Orthot.*, vol. 21, no. 2, pp. 97–99, 2009.
- [18] B. B. Radocy, “Upper-Extremity Prosthetics : Considerations and Designs for Sports and Recreation,” *Clin. Prosthetics Orthot.*, vol. 11, no. 3, pp. 131–153, 1987.
- [19] M. J. Highsmith, S. L. Carey, K. W. Koelsch, C. P. Lusk, and M. E. Maitland, “Design and fabrication of a passive-function, cylindrical grasp terminal device,” *Prosthet. Orthot. Int.*, vol. 33, no. 4, pp. 391–398, 2009.
- [20] S. G. Millstein, H. Heger, and G. A. Hunter, “Prosthetic use in adult upper limb amputees: A comparison of the body powered and electrically powered prostheses,” *Prosthet. Orthot. Int.*, vol. 10, no. 1, pp. 27–34, 1986.
- [21] J. A. Doubler and D. S. Childress, “An analysis of extended physiological proprioception as a prosthesis-control technique,” *J. Rehabil. Res. Dev.*, vol. 21, no. 1, pp. 5–18, 1984.

- [22] S. Micera, J. Carpaneto, and S. Raspopovic, "Control of hand prostheses using peripheral information," *IEEE Rev. Biomed. Eng.*, vol. 3, pp. 48–68, 2010.
- [23] M. Zecca, S. Micera, M. C. Carrozza, and P. Dario, "Control of Multifunctional Prosthetic Hands by Processing the Electromyographic Signal," *Crit. Rev. Biomed. Eng.*, vol. 45, no. 1–6, pp. 383–410, 2002.
- [24] A. Fougner, O. Stavdahl, P. J. Kyberd, Y. G. Losier, and P. A. Parker, "Control of upper limb prostheses: Terminology and proportional myoelectric control: a review," *IEEE Trans. Neural Syst. Rehabil. Eng.*, vol. 20, no. 5, pp. 663–677, 2012.
- [25] J. T. Belter, J. L. Segil, A. M. Dollar, and R. F. Weir, "Mechanical design and performance specifications of anthropomorphic prosthetic hands: a review.," *J. Rehabil. Res. Dev.*, vol. 50, no. 5, pp. 599–618, Jan. 2013.
- [26] S. M. Wurth and L. J. Hargrove, "A real-time comparison between direct control, sequential pattern recognition control and simultaneous pattern recognition control using a Fitts' law style assessment procedure," *J. Neuroeng. Rehabil.*, vol. 11, no. 1, pp. 1–13, 2014.
- [27] K. Englehart and B. Hudgins, "A robust, real-time control scheme for multifunction myoelectric control.," *IEEE Trans. Biomed. Eng.*, vol. 50, no. 7, pp. 848–854, Jul. 2003.
- [28] C. Engineering, "Coapt," 2012. [Online]. Available: <https://coaptengineering.com/technology>. [Accessed: 06-Apr-2023].
- [29] O. S. & C. KGaA, "Myo Plus," 2023. [Online]. Available: https://www.ottobock.com/en-au/Prosthetics/UpperLimb_MyoPlus. [Accessed: 23-May-2023].
- [30] J. M. Hahne *et al.*, "Linear and nonlinear regression techniques for simultaneous and proportional myoelectric control," *IEEE Trans. Neural Syst. Rehabil. Eng.*, vol. 22, no. 2, pp. 269–279, 2014.
- [31] H. J. Hwang, J. M. Hahne, and K. R. Müller, "Real-time robustness evaluation of regression based myoelectric control against arm position change and donning/doffing," *PLoS One*, vol. 12, no. 11, pp. 1–22, 2017.
- [32] A. J. Young, L. H. Smith, E. J. Rouse, and L. J. Hargrove, "A comparison of the real-time controllability of pattern recognition to conventional myoelectric control for discrete and simultaneous movements," *J. Neuroeng. Rehabil.*, vol. 11, no. 1, pp. 1–10, 2014.

- [33] C. Piazza, M. Rossi, M. G. Catalano, A. Bicchi, and L. J. Hargrove, "Evaluation of a Simultaneous Myoelectric Control Strategy for a Multi-DoF Transradial Prosthesis," *IEEE Trans. Neural Syst. Rehabil. Eng.*, vol. 28, no. 10, pp. 2286–2295, 2020.
- [34] S. Salminger *et al.*, "Current rates of prosthetic usage in upper-limb amputees – have innovations had an impact on device acceptance?," *Disabil. Rehabil.*, pp. 1–7, 2020.
- [35] L. V. Mcfarland, S. L. H. Winkler, A. W. Heinemann, M. Jones, and A. Esquenazi, "Unilateral upper-limb loss: Satisfaction and prosthetic-device use in veterans and servicemembers from Vietnam and OIF/OEF conflicts," *J. Rehabil. Res. Dev.*, vol. 47, no. 4, pp. 299–316, 2010.
- [36] E. A. Biddiss and T. T. Chau, "Upper limb prosthesis use and abandonment: A survey of the last 25 years," *Prosthet. Orthot. Int.*, vol. 31, no. 3, pp. 236–257, Sep. 2007.
- [37] H. Burger and Marinček, "Upper limb prosthetic use in Slovenia," *Prosthet. Orthot. Int.*, vol. 18, no. 1, pp. 25–33, 1994.
- [38] K. Østlie, I. M. Lesjø, R. J. Franklin, B. Garfelt, O. H. Skjeldal, and P. Magnus, "Prosthesis use in adult acquired major upper-limb amputees: Patterns of wear, prosthetic skills and the actual use of prostheses in activities of daily life," *Disabil. Rehabil. Assist. Technol.*, vol. 7, no. 6, pp. 479–493, 2012.
- [39] E. Vasluian, I. Van Wijk, P. U. Dijkstra, H. A. Reinders-messelink, and C. K. Van Der Sluis, "Adaptive devices in young people with upper limb reduction deficiencies: Use and satisfaction," *J. Rehabil. Med.*, vol. 47, pp. 1–10, 2015.
- [40] K. Østlie, R. J. Franklin, O. H. Skjeldal, A. Skrondal, and P. Magnus, "Musculoskeletal pain and overuse syndromes in adult acquired major upper-limb amputees," *Arch. Phys. Med. Rehabil.*, vol. 92, no. 12, pp. 1967–1973, 2011.
- [41] L. E. Jones and J. H. Davidson, "Save that arm: a study of problems in the remaining arm of unilateral upper limb amputees," *Prosthet. Orthot. Int.*, vol. 23, pp. 55–58, 1999.
- [42] D. Datta, K. Selvarajah, and N. Davey, "Functional outcome of patients with proximal upper limb deficiency - Acquired and congenital," *Clin. Rehabil.*, vol. 18, no. 2, pp. 172–177, 2004.

- [43] E. Biddiss, D. Beaton, and T. Chau, “Consumer design priorities for upper limb prosthetics,” *Disabil. Rehabil. Assist. Technol.*, vol. 2, no. 6, pp. 346–357, 2007.
- [44] S. L. Carey, D. J. Lura, and M. J. Highsmith, “Systematic literature review,” *J. Rehabil. Res. Dev.*, vol. 52, no. 3, pp. 247–262, 2015.
- [45] F. Cordella *et al.*, “Literature Review on Needs of Upper Limb Prosthesis Users,” *Front. Neurosci.*, vol. 10, no. May, pp. 1–14, May 2016.
- [46] S. Okamoto, H. Nagano, and Y. Yamada, “Psychophysical dimensions of tactile perception of textures,” *IEEE Trans. Haptics*, vol. 6, no. 1, pp. 81–93, 2013.
- [47] M. A. Gonzalez, C. Lee, J. Kang, R. B. Gillespie, and D. H. Gates, “Getting a grip on the impact of incidental feedback from body-powered and myoelectric prostheses,” *IEEE Trans. Neural Syst. Rehabil. Eng.*, vol. 29, pp. 1905–1912, 2021.
- [48] M. Markovic, M. A. Schweisfurth, L. F. Engels, D. Farina, and S. Dosen, “Myocontrol is closed-loop control: Incidental feedback is sufficient for scaling the prosthesis force in routine grasping,” *J. Neuroeng. Rehabil.*, vol. 15:81, pp. 1–11, 2018.
- [49] J. S. Hebert *et al.*, “Quantitative Eye Gaze and Movement Differences in Visuomotor Adaptations to Varying Task Demands Among Upper-Extremity Prosthesis Users,” *JAMA Netw. open*, vol. 2, no. 9, pp. 1–13, 2019.
- [50] P. D. Marasco *et al.*, “Neurobotic fusion of prosthetic touch, kinesthesia, and movement in bionic upper limbs promotes intrinsic brain behaviors,” *Sci. Robot.*, vol. 6, no. 58, pp. 1–13, 2021.
- [51] S. G. Meek, S. C. Jacobsen, and P. P. Gouilding, “Extended physiologic tactation: Design and evaluation of a proportional force feedback system,” *J. Rehabil. Res. Dev.*, vol. 26, no. 3, pp. 53–62, 1989.
- [52] M. Markovic *et al.*, “The clinical relevance of advanced artificial feedback in the control of a multi- functional myoelectric prosthesis,” *J. Neuroeng. Rehabil.*, vol. 15:28, pp. 1–15, 2018.
- [53] M. Aboseria, F. Clemente, L. F. Engels, and C. Cipriani, “Discrete Vibro-Tactile Feedback Prevents Object Slippage in Hand Prostheses More Intuitively Than Other Modalities,” *IEEE Trans. Neural Syst. Rehabil. Eng.*, vol. 26, no. 8, pp. 1577–1584, 2018.

- [54] F. Clemente, M. D’Alonzo, M. Controzzi, B. B. Edin, and C. Cipriani, “Non-Invasive, Temporally Discrete Feedback of Object Contact and Release Improves Grasp Control of Closed-Loop Myoelectric Transradial Prostheses,” *IEEE Trans. Neural Syst. Rehabil. Eng.*, vol. 24, no. 12, pp. 1314–1322, Dec. 2016.
- [55] M. A. Schweisfurth, M. Markovic, S. Dosen, F. Teich, B. Graimann, and D. Farina, “Electrotactile EMG feedback improves the control of prosthesis grasping force,” *J. Neural Eng.*, vol. 13, no. 5, p. 15pp, 2016.
- [56] A. W. Shehata, L. F. Engels, M. Controzzi, C. Cipriani, E. J. Scheme, and J. W. Sensinger, “Improving internal model strength and performance of prosthetic hands using augmented feedback,” *J. Neuroeng. Rehabil.*, vol. 15, no. 1, pp. 1–12, 2018.
- [57] N. Jorgovanovic, S. Dosen, D. J. Djozic, G. Krajoski, and D. Farina, “Virtual grasping: Closed-loop force control using electrotactile feedback,” *Comput. Math. Methods Med.*, vol. 2014, no. Article ID 120357, p. 13pp, Jan. 2014.
- [58] S. Dosen, M. Markovic, K. Somer, B. Graimann, and D. Farina, “EMG Biofeedback for online predictive control of grasping force in a myoelectric prosthesis,” *J. Neuroeng. Rehabil.*, vol. 12, no. 1, p. 55, 2015.
- [59] C. Tejeiro, C. E. Stepp, M. Malhotra, E. Rombokas, and Y. Matsuoka, “Comparison of remote pressure and vibrotactile feedback for prosthetic hand control,” *Proc. IEEE RAS EMBS Int. Conf. Biomed. Robot. Biomechatronics*, pp. 521–525, 2012.
- [60] H. J. B. Witteveen, E. A. Droog, J. S. Rietman, and P. H. Veltink, “Vibro- and electrotactile user feedback on hand opening for myoelectric forearm prostheses,” *IEEE Trans. Biomed. Eng.*, vol. 59, no. 8, pp. 2219–2226, 2012.
- [61] H. J. B. Witteveen, H. S. Rietman, and P. H. Veltink, “Vibrotactile grasping force and hand aperture feedback for myoelectric forearm prosthesis users,” *Prosthet. Orthot. Int.*, vol. 39, no. 3, pp. 204–212, Jun. 2015.
- [62] A. Erwin and F. C. Sup, “A haptic feedback scheme to accurately position a virtual wrist prosthesis using a three-node tactor array,” *PLoS One*, vol. 10, no. 8, p. e0134095, Aug. 2015.
- [63] E. D’Anna *et al.*, “A closed-loop hand prosthesis with simultaneous intraneural tactile and position feedback,” *Sci. Robot.*, vol. 4, no. 27, pp. 1–13, 2019.

- [64] B. Peerdeman *et al.*, “Myoelectric forearm prostheses: State of the art from a user-centered perspective,” *J. Rehabil. Res. Dev.*, vol. 48, no. 6, pp. 719–738, 2011.
- [65] C. Pylatiuk, S. Schulz, and L. Döderlein, “Results of an internet survey of myoelectric prosthetic hand users,” *Prosthet. Orthot. Int.*, vol. 31, no. 4, pp. 362–370, 2007.
- [66] C. Cipriani, J. L. Segil, F. Clemente, R. F. Richard, and B. Edin, “Humans can integrate feedback of discrete events in their sensorimotor control of a robotic hand,” *Exp. Brain Res.*, vol. 232, no. 11, pp. 3421–3429, 2014.
- [67] S. Dosen *et al.*, “Multichannel Electrotactile Feedback With Spatial and Mixed Coding for Closed-Loop Control of Grasping Force in Hand Prostheses,” *IEEE Trans. Neural Syst. Rehabil. Eng.*, vol. 25, no. 3, pp. 183–195, Mar. 2017.
- [68] G. Chai, X. Sui, S. Li, L. He, and N. Lan, “Characterization of evoked tactile sensation in forearm amputees with transcutaneous electrical nerve stimulation,” *J. Neural Eng.*, vol. 12, no. 6, p. 13pp, 2015.
- [69] A. Scarpelli, A. Demofonti, F. Terracina, A. L. Ciancio, and L. Zollo, “Evoking Apparent Moving Sensation in the Hand via Transcutaneous Electrical Nerve Stimulation,” *Front. Neurosci.*, vol. 14, no. June, pp. 1–13, 2020.
- [70] L. Vargas, H. Shin, H. Huang, Y. Zhu, and X. Hu, “Object stiffness recognition using haptic feedback delivered through transcutaneous proximal nerve stimulation,” *J. Neural Eng.*, vol. 17, p. 13pp, 2019.
- [71] E. D’Anna *et al.*, “A somatotopic bidirectional hand prosthesis with transcutaneous electrical nerve stimulation based sensory feedback,” *Sci. Rep.*, vol. 7, no. 1, p. 15pp, 2017.
- [72] F. M. Petrini *et al.*, “Six-Month Assessment of a Hand Prosthesis with Intraneural Tactile Feedback,” *Ann. Neurol.*, vol. 85, no. 1, pp. 137–154, Jan. 2019.
- [73] F. Clemente *et al.*, “Intraneural sensory feedback restores grip force control and motor coordination while using a prosthetic hand,” *J. Neural Eng.*, vol. 16, no. 2, p. 026034, Apr. 2019.
- [74] G. Valle *et al.*, “Comparison of linear frequency and amplitude modulation for intraneural sensory feedback in bidirectional hand prostheses,” *Sci. Rep.*,

vol. 8, no. 1, pp. 1–13, 2018.

- [75] S. N. Flesher *et al.*, “Intracortical microstimulation of human somatosensory cortex,” *Sci. Transl. Med.*, vol. 8, no. 361, p. 361ra141, Oct. 2016.
- [76] G. A. Tabot *et al.*, “Restoring the sense of touch with a prosthetic hand through a brain interface,” *Proc. Natl. Acad. Sci.*, vol. 110, no. 45, pp. 18279–18284, Nov. 2013.
- [77] H. Benz *et al.*, “Upper extremity prosthesis user perspectives on innovative neural interface devices,” *Neuromodulation*, vol. 20 (2), pp. 287–290, 2016.
- [78] S. M. Engdahl, B. P. Christie, B. Kelly, A. Davis, C. A. Chestek, and D. H. Gates, “Surveying the interest of individuals with upper limb loss in novel prosthetic control techniques,” *J. Neuroeng. Rehabil.*, vol. 12, no. 1, pp. 1–11, 2015.
- [79] C. Antfolk, A. Björkman, S. O. Frank, F. Sebelius, G. Lundborg, and B. Rosen, “Sensory feedback from a prosthetic hand based on airmediate d pressure from the hand to the forearm skin,” *J. Rehabil. Med.*, vol. 44, no. 8, pp. 702–707, 2012.
- [80] P. E. Patterson and J. A. Katz, “Design and evaluation of a sensory feedback system that provides grasping pressure in a myoelectric hand,” *J. Rehabil. Res. Dev.*, vol. 29, no. 1, pp. 1–8, 1992.
- [81] E. Battaglia, J. Clark, M. Bianchi, M. Catalano, A. Bicchi, and M. K. O’Malley, “Skin stretch haptic feedback to convey closure information in anthropomorphic, under-actuated upper limb soft prostheses,” *IEEE Trans. Haptics*, vol. 12, no. 4, pp. 508–520, 2019.
- [82] J. Gonzalez, H. Suzuki, N. Natsumi, M. Sekine, and W. Yu, “Auditory display as a prosthetic hand sensory feedback for reaching and grasping tasks,” *Proc. Annu. Int. Conf. IEEE Eng. Med. Biol. Soc. EMBS*, pp. 1789–1792, 2012.
- [83] A. Gibson and P. Artemiadis, “Object discrimination using optimized multi-frequency auditory cross-modal haptic feedback,” *2014 36th Annu. Int. Conf. IEEE Eng. Med. Biol. Soc. EMBC 2014*, pp. 6505–6508, 2014.
- [84] X. Xie *et al.*, “A Review of Smart Materials in Tactile Actuators for Information Delivery,” *C J. Carbon Res. Rev.*, vol. 3, no. 4, p. 38, 2017.
- [85] C. Bermejo and P. Hui, “A survey on haptic technologies for mobile augmented reality,” *arXiv:1709.00698 [cs.HC]*, pp. 1–24, 2017.

- [86] K. A. Kaczmarek, J. G. Webster, P. Bach-y-Rita, and W. J. Tompkins, "Electrotactile and vibrotactile displays for sensory substitution systems," *IEEE Trans. Biomed. Eng.*, vol. 38, no. 1, pp. 1–16, 1991.
- [87] H. Z. Tan, S. Choi, F. W. Y. Lau, and F. Abnoui, "Methodology for maximizing information transmission of haptic devices: A survey," *Proc. IEEE*, vol. 108, no. 6, pp. 945–965, 2020.
- [88] H. Z. Tan, N. L. Durlach, C. M. Reed, and W. M. Rabinowitz, "Information transmission with a multifinger tactual display," *Percept. Psychophys*, vol. 61, no. 6, pp. 993–1008, 1999.
- [89] L. A. Jones, J. Kunkel, and E. Piatetski, "Vibrotactile pattern recognition on the arm and back," *Perception*, vol. 38, no. 1, pp. 52–68, 2009.
- [90] S. Lee and T. Starner, "BuzzWear: Alert perception in wearable tactile displays on the wrist," *Proc. 28th Int. Conf. Hum. Factors Comput. Syst.*, vol. 1, pp. 433–442, 2010.
- [91] H. Y. Chen, J. Santos, M. Graves, K. Kim, and H. Z. Tan, "Tactor localization at the wrist," *EuroHaptics (Lecture Notes Comput. Sci.*, vol. 5024, pp. 209–218, 2008.
- [92] Y. C. Liao, Y. L. Chen, J. Y. Lo, R. H. Liang, L. Chan, and B. Y. Chen, "EdgeVib: Effective alphanumeric character output using a wrist-worn tactile display," *UIST 2016 - Proc. 29th Annu. Symp. User Interface Softw. Technol.*, pp. 595–601, 2016.
- [93] E. D. Z. Chase, A. Israr, P. Preechayasomboon, S. Sykes, A. Gupta, and J. Hartcher-O'brien, "Learning Vibes: Communication Bandwidth of a Single Wrist-Worn Vibrotactile Actuator," *2021 IEEE World Haptics Conf. WHC 2021*, pp. 421–426, 2021.
- [94] C. M. Reed *et al.*, "A Phonemic-Based Tactile Display for Speech Communication," *IEEE Trans. Haptics*, vol. 12, no. 1, pp. 2–17, 2019.
- [95] H. J. B. B. Witteveen, F. Luft, J. S. Rietman, and P. H. Veltink, "Stiffness feedback for myoelectric forearm prostheses using vibrotactile stimulation," *IEEE Trans. Neural Syst. Rehabil. Eng.*, vol. 22, no. 1, pp. 53–61, Jan. 2014.
- [96] A. Ninu, S. Dosen, S. Muceli, F. Rattay, H. Dietl, and D. Farina, "Closed-loop control of grasping with a myoelectric hand prosthesis: Which are the relevant feedback variables for force control?," *IEEE Trans. Neural Syst. Rehabil. Eng.*, vol. 22, no. 5, pp. 1041–1052, 2014.

- [97] J. D. Brown *et al.*, “An exploration of grip force regulation with a low-impedance myoelectric prosthesis featuring referred haptic feedback,” *J. Neuroeng. Rehabil.*, vol. 12, no. 104, pp. 1–17, 2015.
- [98] A. M. De Nunzio *et al.*, “Tactile feedback is an effective instrument for the training of grasping with a prosthesis at low- and medium-force levels,” *Exp. Brain Res.*, vol. 235, no. 8, pp. 2547–2559, 2017.
- [99] A. E. Pena, L. Rincon-gonzalez, J. J. A. Id, and R. J. Id, “Effects of vibrotactile feedback and grasp interface compliance on perception and control of a sensorized myoelectric hand,” *PLoS One*, no. 14:e0210956, pp. 1–22, 2019.
- [100] L. Vargas, H. Huang, Y. Zhu, and X. Hu, “Object Recognition via Evoked Sensory Feedback during Control of a Prosthetic Hand,” *IEEE Robot. Autom. Lett.*, vol. 7, no. 1, pp. 207–214, 2022.
- [101] J. Tchिमino, M. Markovic, J. L. Dideriksen, and S. Dosen, “The effect of calibration parameters on the control of a myoelectric hand prosthesis using EMG feedback,” *J. Neural Eng.*, vol. 18, no. 4, pp. 1–12, 2021.
- [102] J. Tchिमino, J. L. Dideriksen, and S. Dosen, “EMG feedback outperforms force feedback in the presence of prosthesis control disturbance,” *Front. Neurosci.*, vol. 16, no. September, pp. 1–13, 2022.
- [103] P. Mamidanna, J. L. Dideriksen, and S. Dosen, “The impact of objective functions on control policies in closed-loop control of grasping force with a myoelectric prosthesis,” *J. Neural Eng.*, vol. 18, no. 5, 2021.
- [104] P. Mamidanna, J. L. Dideriksen, and S. Dosen, “Estimating speed-accuracy trade-offs to evaluate and understand closed-loop prosthesis interfaces,” *J. Neural Eng.*, vol. 19, no. 056012, 2022.
- [105] A. Chatterjee, P. Chaubey, J. Martin, and N. V. Thakor, “Quantifying prosthesis control improvements using a vibrotactile representation of grip force,” *2008 IEEE Reg. 5 Conf.*, pp. 1–5, 2008.
- [106] M. Bionics, “Luke Arm.” [Online]. Available: <https://www.mobiusbionics.com/luke-arm/>. [Accessed: 06-Apr-2023].
- [107] PSYONIC, “Ability Hand,” 2019. [Online]. Available: <https://www.psyonic.co/abilityhand>. [Accessed: 06-Apr-2023].
- [108] V. Systems, “Vincent Evolution 4,” 2005. [Online]. Available: <https://www.vincentsystems.de/vincent-evolution4>. [Accessed: 06-Apr-

2023].

- [109] M. Azadi and L. A. Jones, "Vibrotactile actuators: Effect of load and body site on performance," *IEEE Haptics Symp. HAPTICS*, pp. 351–356, 2014.
- [110] A. Y. J. Szeto and F. A. Saunders, "Electrocutaneous Stimulation for Sensory Communication in Rehabilitation Engineering," *IEEE Trans. Biomed. Eng.*, vol. BME-29, no. 4, pp. 300–308, Apr. 1982.
- [111] V. Yem and H. Kajimoto, "Comparative Evaluation of Tactile Sensation by Electrical and Mechanical Stimulation," *IEEE Trans. Haptics*, vol. 10, no. 1, pp. 130–134, 2017.
- [112] A. Akhtar, J. Sombeck, B. Boyce, and T. Bretl, "Controlling sensation intensity for electrotactile stimulation in human-machine interfaces," *Sci. Robot.*, vol. 3, no. 17, p. eaap9770, 2018.
- [113] M. Isakovic, J. Malešević, T. Keller, M. Kostić, and M. Štrbac, "Optimization of Semiautomated Calibration Algorithm of Multichannel Electrotactile Feedback for Myoelectric Hand Prosthesis," *Appl. Bionics Biomech.*, vol. 2019, pp. 1–9, Mar. 2019.
- [114] L. A. Jones and N. B. Sarter, "Tactile Displays: Guidance for Their Design and Application," *Hum. Factors J. Hum. Factors Ergon. Soc.*, vol. 50, no. 1, pp. 90–111, 2008.
- [115] S. Parsnejad, S. Dávila-montero, and A. J. Mason, "Use of High-Frequency Pulses to Generate Unique Electrotactile Sensations for Real-Time Feedback in Wearable Sensory Systems," *IEEE Int. Symp. Circuits Syst.*, pp. 3–7, 2020.
- [116] M. Štrbac *et al.*, "Integrated and flexible multichannel interface for electrotactile stimulation," *J. Neural Eng.*, vol. 13, no. 4, pp. 1–16, Aug. 2016.
- [117] M. Solomonow, J. Lyman, and A. Freedy, "Electrotactile two-point discrimination as a function of frequency, body site, laterality, and stimulation codes," *Ann. Biomed. Eng.*, vol. 5, no. 1, pp. 47–60, 1977.
- [118] M. Solomonow, L. Raplee, and J. Lyman, "Electrotactile two point discrimination as a function of frequency, pulse width and pulse time delay," *Ann. Biomed. Eng.*, vol. 6, no. 2, pp. 117–125, 1978.
- [119] M. Isaković *et al.*, "Electrotactile feedback improves performance and facilitates learning in the routine grasping task," *Eur. J. Transl. Myol.*, vol. 26, no. 3, pp. 197–202, 2016.

- [120] G. K. Patel, S. Dosen, C. Castellini, and D. Farina, "Multichannel electro tactile feedback for simultaneous and proportional myoelectric control," *J. Neural Eng.*, vol. 13, no. 5, pp. 1–13, 2016.
- [121] F. Mandrile, D. Farina, M. Pozzo, and R. Merletti, "Stimulation Artifact in Surface EMG Signal: Effect of the Stimulation Waveform, Detection System, and Current Amplitude Using Hybrid Stimulation Technique," *IEEE Trans. Neural Syst. Rehabil. Eng.*, vol. 11, no. 4, pp. 407–415, 2003.
- [122] X. Yi, J. Jia, S. Deng, S. G. Shen, Q. Xie, and G. Wang, "A blink restoration system with contralateral EMG triggered stimulation and real-time artifact blanking," *IEEE Trans. Biomed. Circuits Syst.*, vol. 7, no. 2, pp. 140–148, 2013.
- [123] T. Schauer, R. Salbert, N.-O. Negard, and J. Raisch, "Detection and Filtering of EMG For Assessing Voluntary Muscle Activity During FES," *9th Annu. Conf. Int. FES Soc.*, no. September, pp. 185–187, 2004.
- [124] H. Yeom, H. Park, Y. H. Chang, Y. Park, and K. J. Lee, "Stimulus artifact suppression using the stimulation synchronous adaptive impulse correlated filter for surface EMG application," *J. Electr. Eng. Technol.*, vol. 7, no. 3, pp. 451–458, 2012.
- [125] T. Keller and M. R. Popovic, "Real-time stimulation artifact removal in EMG signals for neuroprosthesis control applications.," *Proc. 6th Annu. IFEES Conf.*, no. June, pp. 4–6, 2001.
- [126] A. H. Arieta, H. Yokoi, T. Arai, and W. Yu, "Study on the effects of electrical stimulation on the pattern recognition for an EMG prosthetic application," *Annu. Int. Conf. IEEE Eng. Med. Biol. - Proc.*, vol. 7 VOLS, no. 16360118, pp. 6919–6922, 2005.
- [127] C. Hartmann *et al.*, "Closed-loop control of myoelectric prostheses with electro tactile feedback: Influence of stimulation artifact and blanking," *IEEE Trans. Neural Syst. Rehabil. Eng.*, vol. 23, no. 5, pp. 807–816, Sep. 2015.
- [128] H. Xu, D. Zhang, J. C. Huegel, W. Xu, and X. Zhu, "Effects of Different Tactile Feedback on Myoelectric Closed-Loop Control for Grasping Based on Electro tactile Stimulation," *IEEE Trans. Neural Syst. Rehabil. Eng.*, vol. 24, no. 8, pp. 827–836, 2016.
- [129] C. Almström, A. Anani, P. Herberts, and L. Körner, "Electrical stimulation and myoelectric control. A theoretical and applied study relevant to prosthesis sensory feedback," *Med. Biol. Eng. Comput.*, vol. 19, no. 5, pp. 645–653,

1981.

- [130] S. Dosen, M. Schaeffer, and D. Farina, “Time-division multiplexing for myoelectric closed-loop control using electrotactile feedback,” *J. Neuroeng. Rehabil.*, vol. 11, no. 1, pp. 1–10, Jan. 2014.
- [131] O. S. & C. KGaA, “bebionic Hand.” [Online]. Available: https://www.ottobock.com/en-us/product/8E7*. [Accessed: 23-May-2023].
- [132] Össur, “iLimb Access.” [Online]. Available: <https://www.ossur.com/en-us/prosthetics/arms/i-limb-access>.
- [133] Ottobock SE & Co. KGaA, “Michelangelo Hand,” 2023. [Online]. Available: <https://www.ottobock.com/en-us/product/8E500>. [Accessed: 23-May-2023].
- [134] M. Schiefer, D. Tan, S. M. Sidek, and D. J. Tyler, “Sensory feedback by peripheral nerve stimulation improves task performance in individuals with upper limb loss using a myoelectric prosthesis,” *J. Neural Eng.*, vol. 13, pp. 1–14, 2016.
- [135] M. A. Schiefer, E. L. Graczyk, S. M. Sidik, D. W. Tan, and D. J. Tyler, “Artificial tactile and proprioceptive feedback improves performance and confidence on object identification tasks,” *PLoS One*, vol. 13, no. 12, pp. 1–18, Dec. 2018.
- [136] E. L. Graczyk, L. Resnik, M. A. Schiefer, M. S. Schmitt, and D. J. Tyler, “Home use of a neural-connected sensory prosthesis provides the functional and psychosocial experience of having a hand again,” *Sci. Rep.*, vol. 8, no. 1, pp. 1–17, 2018.
- [137] C. Cipriani, R. Sassu, M. Controzzi, and M. C. Carrozza, “Influence of the weight actions of the hand prosthesis on the performance of pattern recognition based myoelectric control: Preliminary study,” *33rd Annu. Int. Conf. IEEE EMBS*, pp. 1620–1623, 2011.
- [138] N. M. Malešević *et al.*, “A multi-pad electrode based functional electrical stimulation system for restoration of grasp,” *J. Neuroeng. Rehabil.*, vol. 9, no. 1, pp. 1–12, 2012.
- [139] E. Campbell, A. Phinyomark, and E. Scheme, “Current trends and confounding factors in myoelectric control: Limb position and contraction intensity,” *Sensors (Switzerland)*, vol. 20, no. 6, pp. 1–44, 2020.
- [140] S. Murphy *et al.*, “The relationship between blood flow and motor unit firing

- rates in response to fatiguing exercise post-stroke,” *Front. Physiol.*, vol. 10, no. MAY, pp. 1–14, 2019.
- [141] M. B. I. Reaz, M. S. Hussain, and F. Mohd-Yasin, “Techniques of EMG signal analysis: Detection, processing, classification and applications,” *Biol. Proced. Online*, vol. 8, no. 1, pp. 11–35, 2006.
- [142] M. Atzori *et al.*, “Electromyography data for non-invasive naturally-controlled robotic hand prostheses,” *Sci. Data*, vol. 1, pp. 1–13, 2014.
- [143] N. Celadon, S. Dosen, M. Paleari, D. Farina, and P. Ariano, “Individual finger classification from surface EMG: Influence of electrode set,” *Proc. Annu. Int. Conf. IEEE Eng. Med. Biol. Soc. EMBS*, pp. 7284–7287, 2015.
- [144] N. Jiang, H. Rehbaum, I. Vujaklija, B. Graimann, and D. Farina, “Intuitive, online, simultaneous, and proportional myoelectric control over two degrees-of-freedom in upper limb amputees,” *IEEE Trans. Neural Syst. Rehabil. Eng.*, vol. 22, no. 3, pp. 501–510, 2014.
- [145] H. J. Hermens, B. Freriks, C. Disselhorst-Klug, and G. Rau, “Development of recommendations for SEMG sensors and sensor placement procedures,” *J. Electromyogr. Kinesiol.*, vol. 10, no. 5, pp. 361–374, 2000.
- [146] E. A. Clancy, E. L. Morin, and R. Merletti, “Sampling, noise-reduction and amplitude estimation issues in surface electromyography,” *J. Electromyogr. Kinesiol.*, vol. 12, no. 1, pp. 1–16, 2002.
- [147] H. Türker and H. Sözen, “Surface Electromyography in Sports and Exercise,” *Electrodiagnosis New Front. Clin. Res. up*, vol. 2, pp. 175–194, 2013.
- [148] O. W. Samuel *et al.*, “Intelligent EMG pattern recognition control method for upper-limb multifunctional prostheses: Advances, current challenges, and future prospects,” *IEEE Access*, vol. 7, pp. 10150–10165, 2019.
- [149] R. Menon, G. Di Caterina, H. Lakany, L. Petropoulakis, B. A. Conway, and J. J. Soraghan, “Study on Interaction between Temporal and Spatial Information in Classification of EMG Signals for Myoelectric Prostheses,” *IEEE Trans. Neural Syst. Rehabil. Eng.*, vol. 25, no. 10, pp. 1832–1842, 2017.
- [150] A. Phinyomark, P. Phukpattaranont, and C. Limsakul, “Feature reduction and selection for EMG signal classification,” *Expert Syst. Appl.*, vol. 39, pp. 7420–7431, 2012.
- [151] M. P. Mobarak, J. Manuel, and G. Salgado, “Transient State Analysis of the

- Multichannel EMG Signal Using Hjorth ' s Parameters for Identification of Hand Movements,” *Ninth Int. Multi-Conference Comput. Glob. Inf. Technol.*, pp. 24–30, 2014.
- [152] A. Boschmann, B. Nofen, and M. Platzner, “Improving Transient State Myoelectric Signal Recognition in Hand Movement Classification using Gyroscopes,” *2013 35th Annu. Int. Conf. IEEE Eng. Med. Biol. Soc.*, pp. 6035–6038, 2013.
- [153] I. Mendez *et al.*, “Evaluation of the Myo Armband for the Classification of hand motions,” *Int. Conf. Rehabil. Robot.*, pp. 1211–1214, 2017.
- [154] P. Visconti, F. Gaetani, G. A. Zappatore, and P. Primiceri, “Technical features and functionalities of Myo armband: An overview on related literature and advanced applications of myoelectric armbands mainly focused on arm prostheses,” *Int. J. Smart Sens. Intell. Syst.*, vol. 11, no. 1, pp. 1–25, 2018.
- [155] B. Hudgins, P. Parker, and R. N. Scott, “A new strategy for multifunction myoelectric control,” *IEEE Trans. Biomed. Eng.*, vol. 40, no. 1, pp. 82–94, 1993.
- [156] I. M. Donovan, J. Puchin, K. Okada, and X. Zhang, “Simple space-domain features for low-resolution sEMG pattern recognition,” *Proc. Annu. Int. Conf. IEEE Eng. Med. Biol. Soc. EMBS*, pp. 62–65, 2017.
- [157] N. Celadon *et al.*, “Proportional estimation of finger movements from high-density surface electromyography,” *J. Neuroeng. Rehabil.*, vol. 13, no. 1, pp. 1–19, Dec. 2016.
- [158] J. Malešević, M. Isaković, M. A. Garenfeld, S. Došen, and M. Štrbac, “The Impact of Stimulation Intensity on Spatial Discrimination with Multi-Pad Finger Electrode,” *Appl. Sci.*, vol. 11, no. 21, p. 10231, 2021.
- [159] E. Scheme and K. Englehart, “Electromyogram pattern recognition for control of powered upper-limb prostheses: State of the art and challenges for clinical use,” *J. Rehabil. Res. Dev.*, vol. 48, no. 6, pp. 643–660, 2011.
- [160] D. Yang, Y. Gu, N. V. Thakor, and H. Liu, “Improving the functionality, robustness, and adaptability of myoelectric control for dexterous motion restoration,” *Exp. Brain Res.*, vol. 237, no. 2, pp. 291–311, 2019.
- [161] M. A. Powell, R. R. Kaliki, and N. V. Thakor, “User training for pattern recognition-based myoelectric prostheses: Improving phantom limb movement consistency and distinguishability,” *IEEE Trans. Neural Syst.*

Rehabil. Eng., vol. 22, no. 3, pp. 522–532, 2014.

- [162] A. M. Simon, L. J. Hargrove, B. A. Lock, and T. A. Kuiken, “The Target Achievement Control Test: Evaluating real-time myoelectric pattern recognition control of a multifunctional upper-limb prosthesis,” *J. Rehabil. Res. Dev.*, pp. 619–627, 2011.
- [163] L. Seminara *et al.*, “Dual-Parameter Modulation Improves Stimulus Localization in Multichannel Electrotactile Stimulation,” *IEEE Trans. Haptics*, vol. 13, no. 2, pp. 393–403, 2020.
- [164] E. J. Scheme, B. S. Hudgins, and K. B. Englehart, “Confidence-based rejection for improved pattern recognition myoelectric control,” *IEEE Trans. Biomed. Eng.*, vol. 60, no. 6, pp. 1563–1570, 2013.
- [165] E. Scheme and K. Englehart, “Validation of a selective ensemble-based classification scheme for myoelectric control using a three dimensional Fitts’ law test,” *Neural Syst. Rehabil. Eng. IEEE Trans.*, vol. 21, no. 4, pp. 616–623, 2013.
- [166] E. N. Kamavuako, E. J. Scheme, and K. B. Englehart, “On the usability of intramuscular EMG for prosthetic control: A Fitts’ Law approach,” *J. Electromyogr. Kinesiol.*, vol. 24, no. 5, pp. 770–777, 2014.
- [167] A. Waris, I. Mendez, K. Englehart, W. Jensen, and E. N. Kamavuako, “On the robustness of real-time myoelectric control investigations: A multiday Fitts’ law approach,” *J. Neural Eng.*, vol. 16, no. 2, 2019.

ISSN (online): 2246-1302
ISBN (online): 978-87-7573-681-2

AALBORG UNIVERSITY PRESS